AIChE

Design Under Uncertainty of Hydrocarbon Biorefinery Supply Chains: Multiobjective Stochastic Programming Models, Decomposition Algorithm, and a Comparison Between CVaR and Downside Risk

Berhane H. Gebreslassie, Yuan Yao, and Fengqi You
Dept. of Chemical and Biological Engineering, Northwestern University, IL 60208

DOI 10.1002/aic.13844
Published online May 29, 2012 in Wiley Online Library (wileyonlinelibrary.com).

A bicriterion, multiperiod, stochastic mixed-integer linear programming model to address the optimal design of hydrocarbon biorefinery supply chains under supply and demand uncertainties is presented. The model accounts for multiple conversion technologies, feedstock seasonality and fluctuation, geographical diversity, biomass degradation, demand variation, government incentives, and risk management. The objective is simultaneous minimization of the expected annualized cost and the financial risk. The latter criterion is measured by conditional value-at-risk and downside risk. The model simultaneously determines the optimal network design, technology selection, capital investment, production planning, and logistics management decisions. Multicut L-shaped method is implemented to circumvent the computational burden of solving large scale problems. The proposed modeling framework and algorithm are illustrated through four case studies of hydrocarbon biorefinery supply chain for the State of Illinois. Comparisons between the deterministic and stochastic solutions, the different risk metrics, and two decomposition methods are discussed. The computational results show the effectiveness of the proposed strategy for optimal design of hydrocarbon biorefinery supply chain under the presence of uncertainties. © 2012 American Institute of Chemical Engineers *AIChE J,* 58: 2155–2179, 2012
Keywords: uncertainty, stochastic programming, biomass to liquid, supply chain, risk management, multiobjective optimization

Introduction

Hydrocarbon biorefinery technologies, which convert biomass to hydrocarbon biofuels such as gasoline and diesel, have been considered as promising approaches to overcome the market barrier resulting from the current vehicle technologies and fuel distribution infrastructure.[1,2] Hydrocarbon biofuels can be potentially used without significant changes of the current fuel distribution and utilization, including pipelines, pumping stations, and vehicles. Hydrocarbon biofuels provide vehicle performance similar to or better than their conventional counterparts.[3] The typical biomass to hydrocarbon biofuels conversion pathways are biomass gasification followed by Fischer–Tropsch (FT) synthesis and fast pyrolysis followed by hydroprocessing.[4,5] Renewable fuel standards has put a target of producing 36 billion gallons of biofuels in 2022.[6] Given the relatively short time to achieve the goals and the investment on new infrastructures, it is appealing to investigate infrastructure-compatible fuels. There are existing research works that are devoted to explore the techno-economic feasibilities of future biomass-based hydrocarbon biofuels.[4,5,7,8] However, the techno-economic feasibility of the hydrocarbon biofuel supply chain is subjected to various sources of uncertainty, such as seasonal and geographical fluctuation of biomass supplies, variability in biofuel demands due to unstable economic situations, population growth, the variability of feedstock purchase price and selling price of the hydrocarbon biofuels, and unexpected events. The effects of these uncertainties affect the system's efficiency, eventually leading either to an infeasible supply chain network designs or to a suboptimal performance. Therefore, considering the stochastic nature of the problem and the paramount importance of efficient optimization strategies, which are proved in similar process technologies,[9–12] it is of great importance to develop a more comprehensive stochastic programming model for the optimal design and planning of hydrocarbon biorefinery supply chain that is robust from the economic performance perspective under the presence of uncertainties.

Stochastic programming models that consider the variability of the uncertain parameters typically optimize the expected performance measures of the problem so as to obtain optimal solution that perform well on average of the uncertain events. The standard stochastic programming methods usually do not provide control mechanisms on the unfavorable outcomes. Hence, the solution to the problems is based on the assumption that the decision makers are risk neutral. However, in practice, decision makers may have

Correspondence concerning this article should be addressed to F. You at you@northwestern.edu.

© 2012 American Institute of Chemical Engineers

different attitudes toward the risk associated with the investment on a project under uncertainty. Thus, the supply chain risks should be controlled and managed based on the decision maker preferences. The idea underlying in risk management is incorporating the trade-off between risk and performance measures within the decision-making process.[13,14] This leads to a multiobjective optimization problem in which the expected performance measure of the supply chain and its associated risk are the objectives to be optimized. In this way, coupling of performance measure and risk management tools in multiobjective optimization framework offers an opportunity to reduce the impact of unfavorable events of the uncertain parameters.

The goal of this work is to provide a stochastic programming framework for the design and planning of hydrocarbon biorefinery supply chains under feedstock supply and hydrocarbon biofuels demand uncertainties. The design and planning objective is to minimize the total annualized cost in the face of uncertainty for the entire supply chain that involves harvesting sites, hydrocarbon biorefineries, and demand zones over the entire planning horizon. We propose a stochastic mixed-integer linear programming (MILP) model that integrates decision making across multiple temporal and spatial scales and simultaneously predicts the optimal network design, technology selection, capital investment, production operations, and logistics planning decisions under hydrocarbon biofuels demand and biomass supply uncertainties. The financial risk is controlled and managed at the design stage of the supply chain by incorporating risk metrics such as the conditional value-at-risk (CVaR) and downside risk as one of the objective functions to be minimized. The resulting large scale bicriterion MILP tends to be computationally intractable as the number of scenarios increases. Hence, our modeling framework is complemented by implementing an efficient decomposition approach, which is based on the multicut L-shaped method developed by You and Grossmann,[15] to circumvent the computational burden for large scale optimization.

The capabilities of the proposed modeling framework and solution algorithm are illustrated through four case studies for the optimal design of the hydrocarbon biorefinery supply chain in the State of Illinois that involves of deterministic case, four scenarios, 100 scenarios, and 1000 scenarios. Comparisons between the numerical results of the deterministic and stochastic approaches, between the different risk metrics, and between the standard Benders decomposition and the multicut L-shaped decomposition methods are discussed. Numerical results demonstrate that the proposed strategy allows identifying the optimal values of the first-stage and second-stage variables of the model that leads to a supply chain network design less sensitive to the fluctuations of feedstock supply and product demand, thus improving its robustness in the face of uncertainty. Specifically, according to the uncertain feedstock supply and hydrocarbon biofuels demand, the stochastic programming model varies its choices of transportation network, production capacities, production levels, and the biomass and hydrocarbon biofuels inventories. The results also demonstrate that CVaR is a more effective metric to handle risk than downside risk.

The rest of this article is organized as follows. The review of literatures most relevant to the problem addressed in this work and the novelties of this work are highlighted in the next section. A formal problem statement along with the key assumptions is presented in the Problem Statement section. In the Stochastic Programming section, the MILP mathematical formulation that groups the major constraints and the economic objective is presented. In the Financial Risk Management section, CVaR and downside risk are discussed. The proposed multicut L-shaped decomposition is formally presented in the Solution Algorithm section. In the Case Study section, we present and discuss computational results based on the hydrocarbon biorefinery supply chain for the State of Illinois. Concluding remarks and future directions are presented in the Conclusion section.

Literature Review

In this section, research works most relevant to the problem addressed in this work are reviewed.

Sokhansanj et al.[16] described the development and implementation of a dynamic integrated biomass supply and logistics model to simulate the collection, storage, and transport operations of agricultural biomass supply to biorefinery. With respect to the supply chain optimization of biorefineries, Bowling et al.[17] formulates an optimization model to determine the optimal supply chain, size, operational strategies, location of the biorefinery, and preprocessing hub facilities. Profit is maximized considering the overall sales and the costs for the feedstocks, transportation costs, capital costs, and the operational costs for the facilities. Kim et al.[18] proposed a general MILP model for optimal design of biorefinery that enables the selection of fuel conversion technologies, capacities, biomass locations, and the logistics of transportation from the locations of forestry resources to the conversion sites and then to the final markets. Dunnett et al.[19] proposed a spatially explicit MILP model to explore different spatial infrastructures of lignocellulosic-bioethanol supply chain. They have investigated the cost-optimal system configurations for different technologies, system scale, biomass supply, and ethanol demand distribution, for scenarios specific to European agricultural land and population densities. Zamboni et al.[20] formulated an MILP model for the simultaneous minimization of biomass-based automotive fuel supply chain operating cost and environmental impact. The model takes into account factors that affect the general hydrocarbon biorefinery supply chain such as agricultural practice, biomass supplier allocation, production site locations, capacity assignments, logistics distribution, and transport system optimization. Aksoy et al.[21] investigated four biorefinery technologies for optimal feedstock and facility allocation, economic feasibility, and their economic impacts on Alabama. Elia et al.[22] proposed an MILP model to analyze the United States energy supply chain network for the hybrid coal, biomass, and natural gas to liquids (CBGTL) facilities. The model is developed to determine the optimal locations of CBGTL facilities, the feedstock combination, and size of each facility for minimum overall production cost. The results of the life cycle analysis on each facility of the supply chain network show that the United States fuel demands can be fulfilled with an excess of 50% emissions reduction compared to petroleum-based processes. Corsano et al.[23] proposed a mixed-integer nonlinear programming model for sustainable design and behavior analysis of sugar/ethanol supply chain considering detailed plant performance. They follow simultaneous optimization strategy, which allows the evaluation of several compromises among design and process variables. Akgul et al.[24] presented an MILP model based on the one proposed by Zamboni et al.[20] for

the optimal design of a bioethanol supply chain with the objective of minimizing the total supply chain cost. Their model aims to optimize the locations and scales of the bioethanol production plants, biomass and bioethanol flows between regions, and the number of transport units required for the transfer of these products between regions as well as for local delivery. The model also determines the optimal bioethanol production and biomass cultivation rates. Recently, You and Wang[3] proposed an MILP model to addresses the optimal design and planning of hydrocarbon biorefinery supply chain under economic and environmental criteria. The model is illustrated through a county-level case study for the State of Iowa. The model takes into account diverse conversion pathways and technologies, feedstock seasonality, geographical diversity, biomass degradation, infrastructure compatibility, demand distribution, and government incentives so as to determine the optimal network design, facility location, technology, capital investment, production planning, inventory control, and logistics management decisions. Giarola et al.[25] developed a multiperiod, multiechelon, and spatially explicit multiobjective optimization problem for the design and planning of hybrid first and second generation biorefineries so as to minimize the environmental and financial performances simultaneously. Mele et al.[26] proposed a bicriterion MILP model for the optimal planning of supply chain network of bioethanol and sugar production that considers the simultaneous minimization of the total cost and the environmental performance over the entire life cycle of the supply chain. You et al.[27] proposed a multiobjective MILP model to address the optimal design and planning of cellulosic ethanol supply chains under economic, environmental, and social objectives. The model takes into account the major characteristics of cellulosic ethanol supply chains, including supply seasonality and geographical diversity, biomass degradation, feedstock density, multiple conversion pathways and byproducts, infrastructure compatibility, demand distribution, regional economy, and government incentives. Pareto-optimal designs reveal the trade-off between the economic, environmental, and social dimensions of the sustainable hydrocarbon biorefinery supply chain.

The modeling and optimization strategies reviewed above use the deterministic modeling approach that assumes all problem parameters influencing the optimization task can be perfectly known in advance. This approach provides solutions that perform well at the nominal value of the parameters but can yield poor results for other possible values of the uncertain parameters. In real world applications, however, there are many sources of uncertainty that can influence the decision making in the design and planning of hydrocarbon biorefinery supply chain.[28]

Some research works discuss the effect of uncertainty on the optimal design of biorefinary supply chain. Hytoenen and Stuart[29] investigated the feasibility of integrated biofuel production from several raw materials and diverse technologies under uncertainty. They highlighted the importance of considering technical- and market-based uncertainties in techno-economic assessments thus mitigate risks associated with design decision making. Kim et al.[30] developed a general MILP model to determine the number, location, and size of processing units and the amount of materials to be transported between the various nodes of liquid biorefinary designed network so that the overall expected profit is maximized under uncertainty of parameters that influence the profit. Dal-Mas et al.[31] proposed an MILP model for strategic design and capacity planning of dynamic, spatially explicit, and multiechelon biomass-based ethanol supply chain to assist decision makers and potential investors assessing economic performance and risk on investment of the entire supply chain. The model allows optimizing economic performance and minimizing financial risk on investment by identifying the best network topology in terms of biomass cultivation site locations, ethanol production plant capacities, location, and transport logistics. Marvin et al.[32] proposed an MILP model to determine the optimal biomass harvest, distribution, and biorefineries location and capacity of biomass-to-ethanol supply chain for the Midwest United States. Their model considers five types of agricultural residues for the ethanol production by using dilute acid pretreatment and enzymatic hydrolysis conversion pathways so as to maximize the net present value. They also performed sensitivity of the result to price uncertainty. In their assessment, the results show that with the current parameter variability of the system there is 21.5% chance this industry will not develop.

Uncertainties can be handled by using stochastic programming through incorporating the variability of uncertain parameters at the modeling stage. The use of stochastic programming model allows assessing the supply chain decisions in the space of uncertain parameters before the final decisions are undertaken. The importance of addressing supply chain optimization problems under explicit consideration of uncertainty is reviewed by Sahinidis.[14]

It is imperative to take into account pertinent parameter uncertainty in the optimal design and operations of hydrocarbon biorefinery supply chain. To the best of our knowledge, the optimal design and planning of hydrocarbon biorefinery supply chain under the explicit consideration of feedstock supply and demand uncertainties through multiobjective optimization framework has not been addressed before. The novelty of this work is the effective incorporation of financial risk metrics in the framework of multiobjective optimization under demand and supply uncertainties for the optimal design and planning of hydrocarbon biorefinery supply chains. The other novelty is the implementation of an efficient decomposition approach, which is based on the multicut L-shaped method developed by You and Grossmann,[15] to circumvent the computational challenges for large scale optimization problems.

Process Description

There are a number of process strategies to convert biomass resources into infrastructure-compatible hydrocarbon biofuels (e.g., gasoline, diesel, and jet fuel).[4,5,33] In this work, biomass gasification followed by FT synthesis and fast pyrolysis followed by hydroprocessing technologies are discussed.

Gasification followed by FT synthesis

Gasification followed by FT synthesis technology converts biomass to liquid fuels through the following major operational steps: preprocessing, gasification, syngas cleaning, fuel synthesis, hydroprocessing, power generation, and air separation. The schematic diagram of this process is shown in Figure 1. There are two major gasification technologies: the first option is an oxygen-fed, low-temperature (870°C), nonslagging, fluidized bed gasification and the second option is an

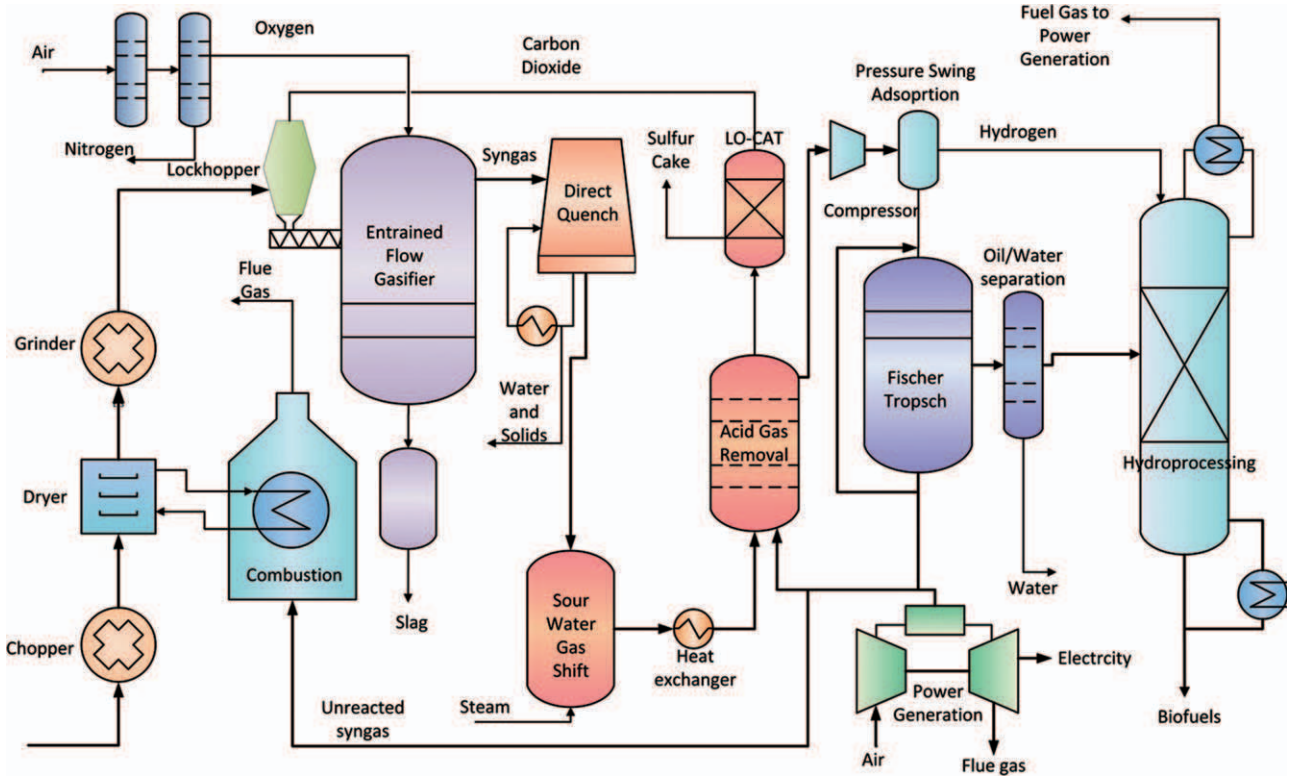

Figure 1. Process flow diagram of the gasification followed by FT synthesis technology.

[Color figure can be viewed in the online issue, which is available at wileyonlinelibrary.com.]

oxygen-fed, high-temperature (1300°C), slagging, entrained flow gasification. The intermediate products from gasification are processed by FT synthesis, where FT synthesis is a process of converting carbon monoxide and hydrogen into liquid hydrocarbons. The high-temperature gasification has high carbon conversion, low tar, and methane content; however, it is accompanied by high capital cost and more complex operation. In contrast, the low-temperature gasification has low capital cost process and high heat transfer rates. However, lower thermal and carbon efficiency are unavoidable disadvantages. In this work, high-temperature gasification is considered.

To enhance the reaction, the biomass collected during harvesting is first dried and grounded into smaller particle sizes according to the type of the gasification. The high-temperature gasification needs a smaller size of 1 mm, whereas low-temperature requires as large as 6 mm. The dried and grounded biomass is then pressurized during gasification with 95% pure oxygen and steam and is converted into flammable gas mixture called raw syngas. Oxygen for gasification is obtained through the air separation unit (ASU). In gasification, the biomass is reacted in the presence of oxygen and produce syngas accompanied by other impurities. The gasification step also includes a combustor, which provides steam for biomass drying. The gasification process is followed by cleaning of the raw syngas from undesired compounds using a cold gas cleaning. Direct water quench cools down the raw syngas to approximately 40°C in low-temperature gasification and 300°C in high-temperature gasification and removes ash and tars content of the syngas. In some plants, cyclones are added to remove particulates before they condense during cooling process. To guarantee the optimal hydrogen to carbon monoxide ratio for the FT synthesis, a water gas shift is installed for low-temperature and a sour water gas shift for high-temperature alternatively.

The clean and adjusted carbon monoxide ratio (2.1:1) syngas is processed through FT synthesis to convert the syngas to hydrocarbon biofuels. The major steps are zinc oxide/activated carbon gas polishing, syngas booster compression, hydrogen separation by pressure swing adsorption, FT synthesis, FT product separation, and distribution of unconverted syngas. Steam methane reforming and water gas shift are additional processes appearing in low-temperature gasification. A zinc oxide and activated carbon sorbent is used to polish the syngas and then the polished syngas stream is compressed to the FT operating pressure, 2500 kPa, and goes through an acid gas removal process. A portion of the syngas goes to a pressure swing adsorption process to provide hydrogen to the hydroprocessing section. The syngas then reacts in FT synthesis to produce hydrocarbon biofuels. The fraction of long chain FT product is further hydrocracked in a hydroprocessing unit to produce hydrocarbon biofuels. Portion of the unconverted syngas is sent back to FT reactor, the combustor, and acid gas removal system. The rest of the unreacted syngas can be combusted in power generation process to provide power for ASU.

Fast pyrolysis followed by hydroprocessing

The schematic of the biomass fast pyrolysis technique to produce renewable gasoline and diesel products is shown in Figure 2. Biomass fast pyrolysis is a technology that uses heat to decompose biomass in the absence of oxygen into gaseous, liquid, and solid products. The major operation steps are: pretreatment of biomass, fast pyrolysis, solid removal, oil recovery, combustion, and hydroprocessing.

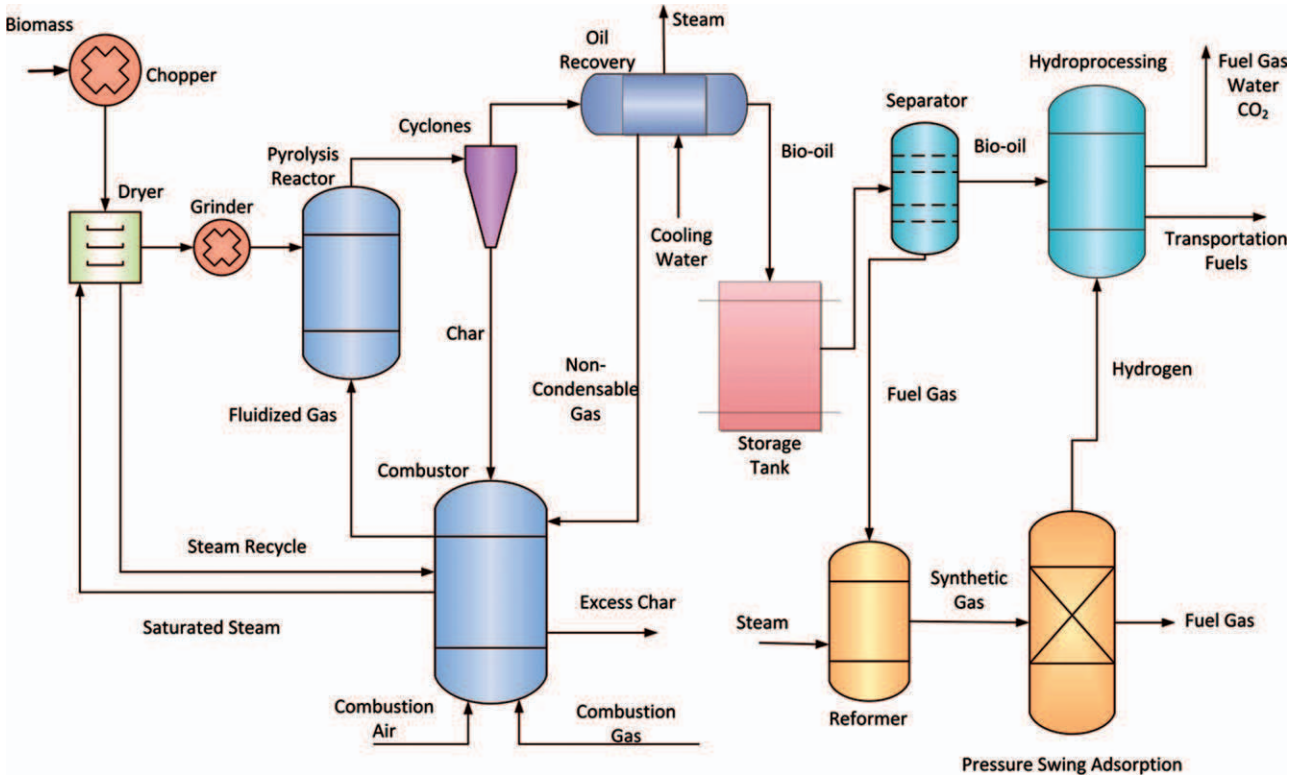

Figure 2. Process flow diagram of the fast pyrolysis + hydroprocessing technology.

[Color figure can be viewed in the online issue, which is available at wileyonlinelibrary.com.]

Similar to pretreatment in gasification, the size of biomass is first reduced to a diameter of 3 mm, and feedstock is dried to less than 7% moisture content. Then the biomass reacts in circulating fluidized bed fast pyrolysis at temperature of 520°C with low residence time. The sizes of pyrolysis particles are much smaller than that in high-temperature gasification, leading to a better performance of cyclones, which are cleaning equipment in the next processing step. Cyclones are able to remove most of entrained char particles. Char particles collected from cyclone are combusted to generate heat. The heat generated can be used for biomass drying and the fast pyrolysis. The vapor is then condensed by an indirect heat exchanger to produce crude bio-oil. The crude oil oxygen level is reduced by converting it into water and carbon dioxides in hydrotreaters. The stable bio-oil is suitable for storage and transportation using the existing infrastructures. Furthermore, the stable bio-oil is separated into lighter and heavy hydrocarbon fractions using consecutive distillation columns. The gasoline range hydrocarbon is collected in gasoline storage and the heavy fraction is sent to the hydrocracker for further breaking down of the long chained hydrocarbons into gasoline and diesel range products. Steam reforming is used to produce hydrogen from the off-gases of hydrotreating and hydrocracking sections and natural gas. The hydrotreating and hydrocracking units use hydrogen from the steam reformer.

Problem Statement

The superstructure of the hydrocarbon biorefinery supply chain taken as a reference in this study is depicted in Figure 3. The network nodes represent a set of biomass feedstock harvesting sites, hydrocarbon biorefineries, and demand zones. The geographical framework includes the region of interest, which can be divided into a set of potential locations. Each location is a potential feedstock biomass supplier, a possible hydrocarbon biorefinary location, and a hydrocarbon biofuels demand zone.

The problem can be formally stated as follows: the given parameters are presented below:

- The planning horizon that is divided into a number of time periods of known duration.
- Hydrocarbon biorefinery life time in terms of years.
- Set of biomass feedstocks, the major properties of each type of feedstock, biomass deterioration rate, feedstock distribution that reflects variation due to seasonality, and geographical and weather conditions.
- Set of available production technologies and associated yield of each type of biofuel product.
- Set of potential harvesting sites, plant locations, and demand zones along with the associated demand distribution that follows known probability distribution that reflects the fluctuation of demand due to economic, behavioral, or other factors.
- Capacity levels of hydrocarbon biorefineries, upper and lower bounds of hydrocarbon biorefinery capacities for each capacity level, conversion technology, and safety storage level.
- Costs associated with the network operation (production, transportation, and inventory costs).
- Government incentives, both construction and volumetric incentives.
- The distance between nodes of the supply chain network.
- Weight capacity of biomass transportation in each time period.

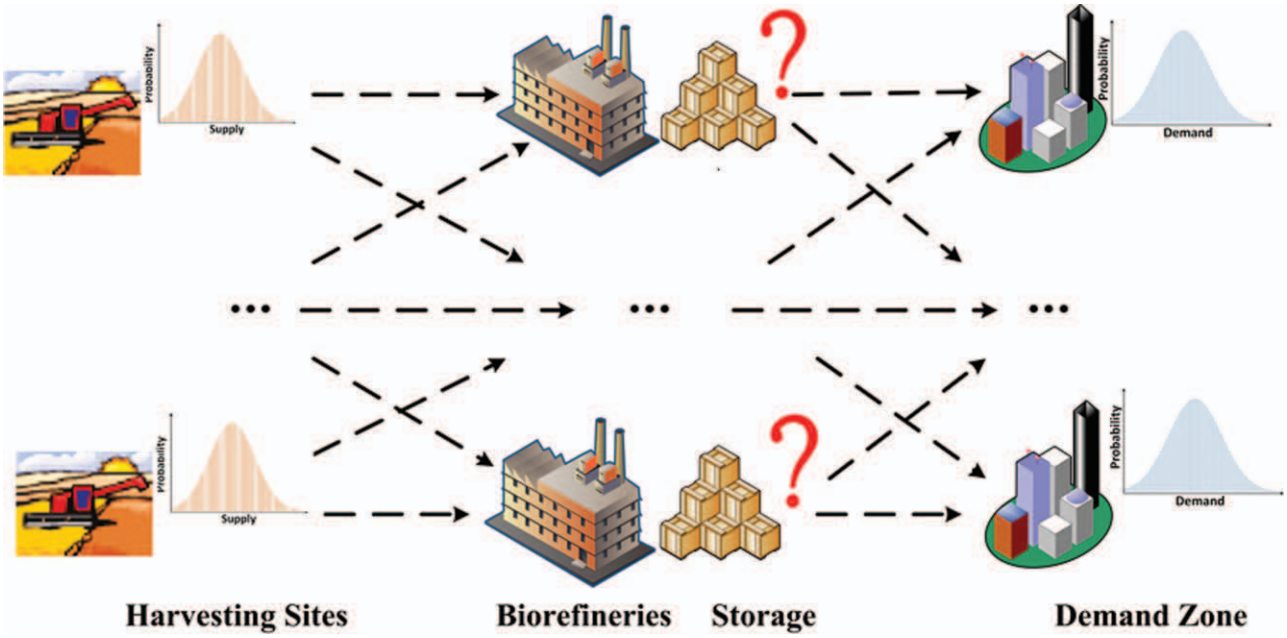

Figure 3. Hydrocarbon biorefinery supply chain superstructure.

[Color figure can be viewed in the online issue, which is available at wileyonlinelibrary.com.]

The goal of this problem is minimizing the total expected annual cost and the financial risk associated with the optimal design of the hydrocarbon supply chain and determining the following decision variables:

- The number, capacities, locations, and technology selections of hydrocarbon biorefinery plants.
- Production rates of plants, inventory levels at harvesting sites and at plant locations in each time period.
- Shipment quantities of biomass feedstocks between harvesting sites and plant locations at each time period.
- Shipment quantities of hydrocarbon biofuels between plants and demand zones at each time period; quantities of hydrocarbon biofuel demand satisfied in each demand zone at each time period.

The following assumptions are made in the hydrocarbon biofuels supply chain modeling:

- Demand zone: The model is developed to design a network capable of satisfying a given hydrocarbon biofuels demand of each demand zone in each time period. Each demand zone can order one or more types of hydrocarbon biofuels. The demand may be assumed to be known as *a priori*. A demand zone can be served by more than one hydrocarbon biorefineries.
- Production zone: biomass can be supplied from one or more harvesting sites. Hydrocarbon biofuels can be supplied to more than one demand zones.
- Multiperiod: the hydrocarbon biorefinery supply chain design covers a fixed time horizon divided in several periods of time accounting for fluctuation of feedstock supply and hydrocarbon biofuels demand.
- Uncertainty: The feedstock supply and hydrocarbon biofuels demand are considered as uncertain parameters. The rest of the parameters involved in the supply chain design and planning are assumed to be deterministic. However, the model is general enough to be extended to account for other parameter uncertainties.

Stochastic Programming Model

One popular approach of modeling under uncertainty is the two-stage stochastic programming approach. It is defined by an outer master problem (deterministic model) dealing with first-stage variables and the inner stochastic programming model (recourse model) dealing with the uncertain parameter realization.[14,34] Two-stage stochastic programming that addresses different classes of problems can be found in the open literature databases. For example, process design problems,[35,36] planning and scheduling,[37,38] and supply chain management.[39,40]

Two-stage approach

We apply a two-stage stochastic programming approach to obtain the optimal design of the hydrocarbon biorefinery supply chain network under uncertainty and integrate it into a multiperiod planning model. This problem can be modeled as a multistage stochastic programming model; however, we only consider a two-stage approach to reduce computational complexity. In the two-stage stochastic programming approach, the decision variables of an optimization problem under uncertainty are divided into two sets. The first-stage variables are those which have to be decided before the actual realization of the uncertain parameters. For example, before the actual realization of the uncertain parameters, decisions on production and inventory for the current time period are made "here and now" at the first stage while decisions for the rest of time periods have to "wait-and-see" after the true value of uncertainties are realized. Once the uncertain events are realized, further design or operational improvements can be made by selecting the values of the second-stage, or recourse, variables. Because of the uncertainty, the second-stage cost is an uncertain variable. The objective is to choose the first-stage variables in a way that the sum of the first-stage cost and the expected value of the second-stage cost is minimized.

Mathematical formulation

The mathematical formulation of the multiperiod stochastic programming model is developed so as to allow the costs, levels of production, and inventory decisions to change with time and uncertain event realization. Model constraints are divided into first-stage constraints that include constraints 1–7 and 20, and second stage including constraints 8–19 and 21–27. The economic objective function is presented in Eq. 28. The first-stage decision variables are annual production capacity ($\text{capj}_{j,q,r}$), government incentives for construction of biorefineries (incj_j), total capital investment of installing biorefineries (tcapj_j), and fixed operations and maintenance (O&M) cost of hydrocarbon biorefinery (tcfpj_j). The second-stage decision variables are biomass harvest ($\text{bmp}_{b,i,t,s}$), biomass shipment ($\text{fij}_{b,i,j,m,t,s}$) and product transportation ($\text{fjk}_{j,k,p,m,t,s}$), inventory levels ($\text{sbj}_{b,j,t,s}$ and $\text{spj}_{j,p,t,s}$), biomass consumption ($\text{wbj}_{b,j,q,t,s}$), hydrocarbon biofuels production ($\text{wpj}_{j,p,q,t,s}$), and the amount of hydrocarbon biofuels sold ($\text{sold}_{k,p,t,s}$). The definitions of sets, variables, and parameters of the model are given at the end of this article.

First-Stage Constraints. A binary variable, $x_{j,q,r}$, is introduced to enforce the selection of conversion technology, capacity level, and hydrocarbon biorefinery location in the following constraints

$$\sum_q \sum_r x_{j,q,r} \le 1, \qquad \forall j \in J \tag{1}$$

$$\sum_j \sum_r x_{j,q,r} \le NJ_q, \qquad \forall q \in Q \tag{2}$$

where $x_{j,q,r}$ is equal to 1 if a biorefinery with technology q and capacity level r is constructed at production site j and NJ_q is the maximum allowable number of integrated biorefineries with technology q. Constraint 1 states that at most one type of technology and capacity level can be chosen at any given site j. Constraint 2 enforces the upper bound on the total number of biorefineries with technology q.

The annual production capacity (in terms of gallons of gasoline equivalent) of hydrocarbon biorefinery j for product p at level r is constrained in the following equations

$$\text{PRJ}_{j,q,r-1} \cdot x_{j,q,r} \le \text{capj}_{j,q,r} \le \text{PRJ}_{j,q,r} \cdot x_{j,q,r}, \quad \forall j \in J, q \in Q, r \in R \tag{3}$$

where $\text{PRJ}_{j,q,r}$ is the maximum capacity of hydrocarbon biorefinery j with technology q and capacity lever r. Constraint 3 also enforces zero value of the production capacity of technology q at production level r if no biorefinery is constructed in site j.

The total capital investment of installing hydrocarbon biorefinery j is modeled by an interpolated piecewise linear curve for each capacity level.[19]

$$\text{tcap}j_j = \sum_q \sum_r \left[\text{CRJ}_{j,q,r-1} \cdot x_{j,q,r} + \left(\text{capj}_{j,q,r} - \text{PRJ}_{j,q,r-1} \cdot x_{j,q,r} \right) \cdot \left(\frac{\text{CRJ}_{j,q,r} - \text{CRJ}_{j,q,r-1}}{\text{PRJ}_{j,q,r} - \text{PRJ}_{j,q,r-1}} \right) \right] \qquad \forall j \in J \tag{4}$$

where $\text{CRJ}_{j,q,r}$ and $\text{PRJ}_{j,q,r}$ are total capital investment and upper bound of capacity of hydrocarbon biorefinery j with technology q and capacity level r, respectively. $\text{CRJ}_{j,q,r}$ is a given parameter. If the binary variable $x_{j,q,r}$ takes 0 for all technology q and capacity level r in site j, the total capital investment cost of installing hydrocarbon biorefinery j equals 0.

The fixed annual O&M cost of hydrocarbon biorefinery j (tcfpj_j) can be modeled in a similar way

$$\text{tcfpj}_j = \sum_q \left\{ \text{CFJ}_{j,q} \cdot \sum_r \left[\text{CRJ}_{j,q,r-1} \cdot x_{j,q,r} + \left(\text{capj}_{j,q,r} - \text{PRJ}_{j,q,r-1} \cdot x_{j,q,r} \right) \cdot \left(\frac{\text{CRJ}_{j,q,r} - \text{CRJ}_{j,q,r-1}}{\text{PRJ}_{j,q,r} - \text{PRJ}_{j,q,r-1}} \right) \right] \right\} \quad \forall j \in J \tag{5}$$

where $\text{CFJ}_{j,q}$ is fixed annual O&M cost that is a given parameter as the percentage of the total investment cost of hydrocarbon biorefinery j with conversion technology q, and its value depends on the type of technology chosen.

If hydrocarbon biorefinery j is installed, the government incentives received for construction should be less than a certain percentage (INCP) of total capital investment and maximum allowable incentive (INCM).[19] The definition of such incentives is given by the following two constraints

$$\text{incj}_j \le \text{INCM} \cdot \sum_q \sum_r x_{j,q,r}, \qquad \forall j \in J \tag{6}$$

$$\text{incj}_j \le \text{INCP} \cdot \text{tcapj}_j, \qquad \forall j \in J \tag{7}$$

Constraint 6 guarantees that government incentives will be 0 if no biorefinery is constructed at site j.

Second-Stage Constraints. The total amount of biomass type b collected from harvesting site i at time period t for scenario s ($\text{bmp}_{b,i,t,s}$) should not exceed the available amount ($\text{BA}_{b,i,t,s}$).

$$\text{bmp}_{b,i,t,s} \le \text{BA}_{b,i,t,s}, \qquad \forall b \in B, i \in I, t \in T, s \in S \tag{8}$$

The value of parameter $\text{BA}_{b,i,t,s}$ at different harvesting sites and time periods for different biomass types and scenarios can reflect seasonality, harvesting windows, and geographical availability of different biomass feedstocks.

Because no feedstock is stored in harvesting sites, the total amount of biomass harvested should be equal to the amount shipped to all biorefineries. The total transportation amount of biomass feedstock from harvesting site i to biorefinary site j with transportation mode m in time period t is constrained by the corresponding transportation capacity in weight as shown in constraint 9.

$$\text{bmp}_{b,i,t,s} = \sum_j \sum_m \text{fij}_{b,i,j,m,t,s}, \quad \forall b \in B, i \in I, t \in T, s \in S \tag{9}$$

where $\text{fij}_{b,i,j,m,t,s}$ is the amount of biomass type b on a mass basis shipped from harvesting site i to biorefinery j with transportation mode m at time period t for scenario s.

As no feedstock has been dried before transportation from harvesting sites to biorefineries, moisture content (MC_b) is considered through constraint 10. Constraint 10 also takes into account the intermodal transportation of multiple feedstocks with the same transportation link through the factor ρ_b, which is the mass quantity of standard dry biomass for 1 dry ton of biomass type b.

$$\sum_b \frac{\rho_b \cdot \mathrm{fij}_{b,i,j,m,t,s}}{1-\mathrm{MC}_b} \le \mathrm{WCIJ}_{i,j,m,t},\ \forall i \in I, j \in J, m \in M, t \in T, s \in S \quad (10)$$

where $\mathrm{WCIJ}_{i,j,m,t}$ is weight capacity for the transportation of biomass from harvesting site i to hydrocarbon biorefinery j with transportation mode m in time period t.

The mass balance regulates the flow interactions among the hydrocarbon biorefinery supply chain and must be satisfied for every biomass type b, hydrocarbon biofuel product type p, in each potential biorefinery location, harvesting site, and demand zone in time period t for each scenario s. The mass balance of biomass feedstock b in biorefinery j at time period t for scenario s is given by the following constraint

$$\sum_i \sum_m \mathrm{fij}_{b,i,j,m,t,s} + (1-\varepsilon_{b,t}) \cdot \mathrm{sbj}_{b,j,t-1,s} = \sum_q \mathrm{wbj}_{b,j,q,t,s} + \mathrm{sbj}_{b,j,t,s}, \quad \forall b \in B, j \in J, t \ge 2, s \in S \quad (11)$$

where $\mathrm{sbj}_{b,j,t,s}$ is the inventory level of biomass type b in hydrocarbon biorefinery j at time period t for scenario s, $\mathrm{wbj}_{b,j,q,t,s}$ is the total amount of biomass type b used for the production of liquid transportation fuel by conversion technology q in hydrocarbon biorefinery j at time period t for scenario s. $\varepsilon_{b,t}$ is considered as a percentage of biomass type b deteriorated in storage facility at time period t. It can reflect the level of degradation of biomass feedstock. The left-hand side of the constraint sums up the amount of biomass feedstock type b shipped from all harvesting sites with all possible transportation mode m and inventory level at previous time period $t-1$ after degradation. This summation equals to the right-hand, that is, usage of this type of biomass plus its inventory at the end of this time period t.

Inventory balance is modeled in a "cyclic" way which means the inventory level at the beginning of the year is equal to the level at the end of the year. Also, biomass degradation is taken into account in this case. Such a relationship is given by the following constraint

$$\sum_i \sum_m \mathrm{fij}_{b,i,j,m,t=1,s} + (1-\varepsilon_{b,t=1}) \cdot \mathrm{sbj}_{b,j,t=|T|,s} = \sum_q \mathrm{wbj}_{b,j,q,t=1,s} + \mathrm{sbj}_{b,j,t=1,s},\ \forall b \in B, j \in J, s \in S \quad (12)$$

The mass balance of liquid transportation fuel p produced at biorefinery j at time period t for scenario s is expressed by the following constraints

$$\sum_q \mathrm{wpj}_{j,p,q,t,s} + \mathrm{spj}_{j,p,t-1,s} = \sum_k \sum_m \mathrm{fjk}_{j,k,p,m,t,s} + \mathrm{spj}_{j,p,t,s}, \quad \forall j \in J, p \in P, t \ge 2, s \in S \quad (13)$$

In constraint 13, $\mathrm{wpj}_{j,p,q,t,s}$ is the amount of fuel product type p produced by conversion technology q in hydrocarbon biorefinery j at time period t for scenario s. $\mathrm{spj}_{j,p,t,s}$ is the inventory level of fuel product p in hydrocarbon biorefinery j at time period t for scenario s. $\mathrm{fjk}_{j,k,p,m,t,s}$ is the amount of liquid fuel p shipped from hydrocarbon biorefinery j to demand zones k with transportation mode m in time period t for scenario s. Similarly, "cyclic" inventory balance is applied to liquid fuel product that is given by constraint 14.

$$\sum_q \mathrm{wpj}_{j,p,q,t=1,s} + \mathrm{spj}_{j,p,t=|T|,s} = \sum_k \sum_m \mathrm{fjk}_{j,k,p,m,t=1,s} + \mathrm{spj}_{j,p,t=1,s}, \quad \forall j \in J, p \in P, s \in S \quad (14)$$

The amount of fuel product p produced in hydrocarbon biorefinery j with conversion technology q at time period t for scenario s ($\mathrm{wpj}_{j,p,q,t,s}$) should not exceed the annual production capacity ($\mathrm{capj}_{j,q,r}$) times the duration of time period t (H_t) divided by the duration of time of a year (HY). Lower bound of the total production amount is enforced by introducing a minimum utilization capacity rate ($\theta_{j,q}$). Thus, the production capacity constraints are given by

$$\theta_{j,q} \cdot \frac{H_t}{\mathrm{HY}} \cdot \sum_r \mathrm{capj}_{j,q,r} \le \sum_p \phi_p \cdot \mathrm{wpj}_{j,p,q,t,s} \le \frac{H_t}{\mathrm{HY}} \cdot \sum_r \mathrm{capj}_{j,q,r}, \quad \forall j \in J, q \in Q, t \in T, s \in S \quad (15)$$

where ϕ_p is gasoline-equivalent gallons (GEG) of one gallon of liquid fuel product p.

The mass balance between the production amount of fuel product p and biomass consumption amount at biorefinery j with technology q at time period t for scenario s is enforced by the following constraint

$$\mathrm{wpj}_{j,p,q,t,s} = \sum_b \alpha_{b,p,q} \cdot \mathrm{wbj}_{b,j,q,t,s}, \quad \forall j \in J, p \in P, q \in Q, t \in T, s \in S \quad (16)$$

where $\alpha_{b,p,q}$ is the yield of fuel product p from unit quantity of biomass type b using conversion technology q.

The inventory level of biomass type b in hydrocarbon biorefinery j at time period t for scenarios s has a lower bound that is safety stock level given by following constraint

$$\mathrm{sbj}_{b,j,t,s} \ge \frac{\mathrm{SJ}_{j,t}}{H_t} \cdot \sum_q \mathrm{wbj}_{b,j,q,t,s}, \quad \forall b \in B, j \in J, t \in T, s \in S \quad (17)$$

where the right-hand-side of constraint is the safety stock inventory that should be hold to cover the production shortage in the same biorefinery at time period t. The inventory level of biomass should be higher than or equal to the safety stock level to avoid possible supply disruption. Strictly speaking, the optimal safety stock level should be obtained through a stochastic inventory model that integrates demand and supply uncertainty with supply chain design and operations.[41–44] Because of the complexity of the stochastic inventory approach, we use an empirical approach that relates the safety stock level to the amount of feedstock consumption over a safety period $\mathrm{SJ}_{j,t}$.

For any scenario s, the total hydrocarbon biofuel p sold at demand zone k in time period t ($\mathrm{sold}_{k,p,t,s,}$) should be able to satisfy the total amount of hydrocarbon biofuels transported to the same demand zone from all biorefineries with all the transportation modes. $\mathrm{sold}_{k,p,t,s}$ should also meet the requirement of demand at the same zone and is constrained as follows.

$$\sum_j \sum_m \mathrm{fjk}_{j,k,p,m,t,s} = \mathrm{sold}_{k,p,t,s} \quad \forall k \in K, p \in P, t \in T, s \in S \quad (18)$$

$$\mathrm{sold}_{k,p,t,s} + \mathrm{slack}_{k,p,t,s} \ge \mathrm{DEM}_{k,p,t,s}, \quad \forall k \in K, p \in P, t \in T, s \in S \quad (19)$$

where $\mathrm{DEM}_{k,p,t,s}$ is the lower bound of demand for transportation fuel product p at demand zone k at time period t for scenarios s. $\mathrm{slack}_{k,p,t,s}$ is the amount of demand of product type p at demand zone k at time period t for scenario s that are not satisfied.

Economic Objective. Our model considers the feedstock supply and hydrocarbon biofuel demand as uncertain parameters. They are described through a set of scenarios with known distribution. As a result, the total annualized cost associated with design and planning of the hydrocarbon biofuels supply chain is not a single nominal value; instead it is a stochastic variable that follows a discrete probability function. In this regard, the optimization method must identify a set of designs and planning of the supply chain network that simultaneously minimizes the expected annualized cost and the financial risk level. The expected annual cost formulation is presented in this section.

The total expected annualized cost includes the total cost of first stage and the expected cost of second stage. The first-stage cost refers to total capital cost that is the product of investment discount and the difference between total capital investment and government incentive. The relationship is represented by the following constraint

$$C^{\mathrm{capital}} = \frac{\mathrm{IR}\cdot(1+\mathrm{IR})^{\mathrm{NY}}}{(1+\mathrm{IR})^{\mathrm{NY}}-1}\cdot\left(\sum_j \mathrm{tcapj}_j - \sum_j \mathrm{incj}_j\right) \tag{20}$$

The second-stage cost is the summation of expected cost of biomass feedstock acquisition cost, the local distribution cost of liquid fuel product, the production cost, the transportation and storage cost, minus the government incentives. The production cost is consisted of fixed annual O&M cost in first stage and the net variable cost that is the product of net unit production cost ($\mathrm{CPJ}_{j,p,q}$) and amount of biomass. The transportation cost is expressed in terms of distance-fixed cost and distance-variable cost. The expenses of storing biomass and liquid fuel product are both taken into account in storage cost. The government incentive in second stage is equal to the product of volumetric production inventive of liquid transportation fuel p sold to demand zone k ($\mathrm{INCV}_{k,p}$) and the amount of p sold to the same zone at time period t for scenario s. The above costs are given by the following constraints

$$C_s^{\mathrm{acquisition}} = \sum_b\sum_i\sum_t \mathrm{CBM}_{b,i,t}\cdot \mathrm{bmp}_{b,i,t,s} \tag{21}$$

$$C_s^{\mathrm{distribution}} = \sum_k\sum_p\sum_t \mathrm{CLD}_{k,p}\cdot \mathrm{sold}_{k,p,t,s} + \sum_k\sum_p\sum_t \mathrm{PCD}\cdot \mathrm{slack}_{k,p,t,s} \tag{22}$$

$$C_s^{\mathrm{production}} = \sum_j \mathrm{tcfpj}_j + \sum_j\sum_p\sum_q\sum_t \mathrm{CPJ}_{j,p,q}\cdot \mathrm{wpj}_{j,p,q,t,s} \tag{23}$$

$$C_s^{\mathrm{transportation}} = \sum_b\sum_i\sum_j\sum_m\sum_t \left(\mathrm{DFCB}_{b,m} + \mathrm{DVCB}_{b,m,t}\cdot\mathrm{DSIJ}_{i,j,m}\right)\cdot \mathrm{fij}_{b,i,j,m,t,s} + \sum_j\sum_k\sum_p\sum_m\sum_t \left(\mathrm{DFCP}_{m,p} + \mathrm{DVCP}_{m,p,t}\cdot \mathrm{DSJK}_{j,k,m}\right)\cdot \mathrm{fjk}_{j,k,p,m,t,s} \tag{24}$$

$$C_s^{\mathrm{storage}} = \sum_b\sum_j\sum_t H_t\cdot \mathrm{HBJ}_{b,j,t}\cdot \mathrm{sbj}_{b,j,t,s} + \sum_j\sum_p\sum_t H_t\cdot \mathrm{HPJ}_{j,p,t}\cdot \mathrm{spj}_{j,p,t,s} \tag{25}$$

$$C_s^{\mathrm{Incentive}} = \sum_k\sum_p\sum_t \mathrm{INCV}_{k,p}\cdot \mathrm{sold}_{k,p,t,s} \tag{26}$$

The total expected cost can be expressed as the summation of the first-stage cost and the expected second-stage cost. Because the scenarios follow discrete distribution, the expected second-stage cost is given by the sum of the product of scenario probability (p_s) and second-stage cost (Cost_s^{2stg}) over all scenario s.

$$\mathrm{Cost}_s^{2stg} = C_s^{\mathrm{acquisition}} + C_s^{\mathrm{distribution}} + C_s^{\mathrm{production}} + C_s^{\mathrm{transportation}} + C_s^{\mathrm{storage}} - C_s^{\mathrm{incentive}} \tag{27}$$

$$E[\mathrm{Cost}] = \mathrm{Cost}^{\mathrm{capital}} + \sum\nolimits_{s\in S} p_s \mathrm{Cost}_s^{2stg} \tag{28}$$

Risk Management Models

To control and manage risk at the optimal design of the hydrocarbon biorefinery supply chain, CVaR proposed by Uryasev and Rockafellar [45,46] and downside risk proposed by Eppen and Martin[47] are introduced to the model. Application of downside risk to handle financial risk can be viewed at You et al.[40] and Gebreslassie et al.[48] Application for CVaR can be refered to Verderame and Floudas[34] and Carneiro et al.[49]

In the stochastic programming model, which relies on formulating a single objective optimization problem, the total expected cost is optimized and the solutions are optimal on average of all the scenarios. In this case, the expected cost is assumed as a risk-neutral objective function that cannot control or manage the risks explicitly. On the other hand, some decision makers are risk-averse and would like to manage the risks and improve the economic objective simultaneously. This requires extending the aforementioned stochastic programming model to risk management. The fundamental idea of risk management is incorporating the trade-off between financial risk and expected cost into the decision-making procedure of the supply chain network design. This leads to the formulation of a multiobjective optimization problem, in which the expected economic performance and a specific risk metric are the objective functions to be optimized. Hence, we need to define the financial risk metrics. For comparison purpose, we consider two popular methods to measure the financial risk: downside risk and CVaR. They are briefly presented below.

Managing downside risk

Managing the downside risk using the probabilistic approaches emphases on the extremes of the cost spreads as shown in Figure 4. This approach minimizes the risk associated with scenarios whose costs exceed certain threshold (Ω) suggested by decision makers at the expense of lowering the probability of low-cost scenarios. The possible way of handling the financial risk is to use the definition of downside risk.[40] Mathematically, this metric can be determined as follows:

$$\psi_s \geq \mathrm{Cost}_s - \Omega, \quad \psi_s \geq 0, \quad s\in S \tag{29}$$

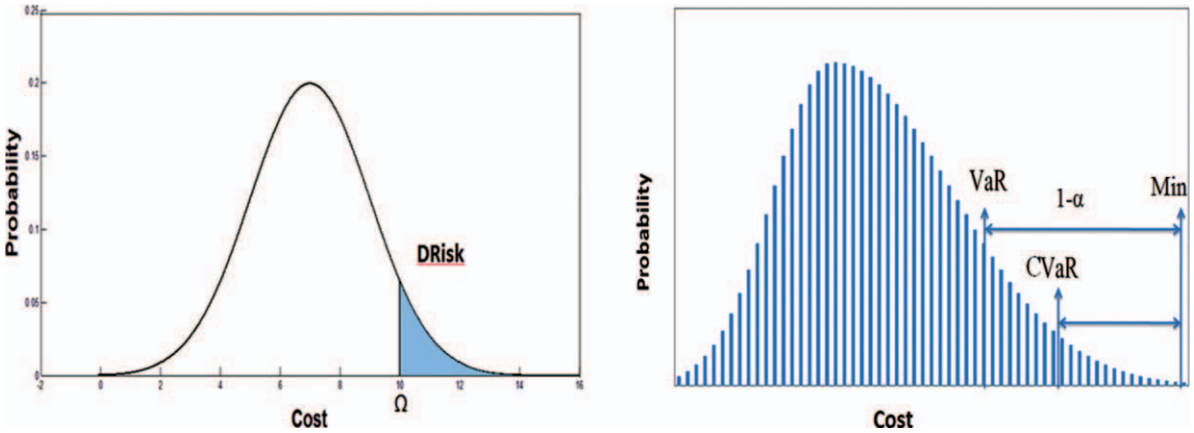

Figure 4. Definition of downside risk and CVaR.

[Color figure can be viewed in the online issue, which is available at wileyonlinelibrary.com.]

$$\text{Cost}_s = \text{Cost}^{\text{capital}} + \text{Cost}_s^{2stg} \tag{30}$$

where Cost_s is the total annualized cost of the hydrocarbon biorefinery supply chain in scenario s, which is given by the sum of the total capital cost ($\text{Cost}^{\text{capital}}$) and second-stage cost (Cost_s^{2stg}) in Eq. 30. $\psi_s(x,\Omega)$ is a non-negative variable that measures deviation of scenario cost from a target Ω. If the cost of scenario s is less than Ω then $\psi_s(x,\Omega)$ takes 0. Therefore, downside risk ($\text{DRisk}(x,\Omega)$) relating to target Ω is defined as the expected value of the non-negative variable ($\psi_s(x,\Omega)$). The downside risk is defined as follows

$$\text{DRisk}(x,\Omega) = \sum_{s\in S} p_s \cdot \psi_s(x,\Omega) \tag{31}$$

Thus, the downside risk management model is given below

$$\min E[Cost] = Cost^{capital} + \sum\nolimits_{s\in S} p_s Cost_s^{2stg} \tag{28}$$

$$\min\ \text{DRisk}(x,\Omega) = \sum_{s\in S} p_s \cdot \psi_s(x,\Omega) \tag{32}$$

$$\text{s.t.}\ \ \psi_s \geq \text{Cost}_s - \Omega, \quad \psi_s \geq 0, \quad s \in S \tag{33}$$

Constraints 1–27

This model has two objectives, minimizing total expected cost 28 and minimizing the downside risk in Eq. 32, subjected to constraints 33 and 1–27. ε-Constraint method can be applied for solving the multiobjective optimization model and the solution forms a Pareto curve.

Managing CVaR

CVaR management is another approach of risk management. Instead of fixing a target cost Ω, a given quantile $\alpha \in (0,1)$ is considered. Then two non-negative variables, value-at-risk (VaR) and deviation (ϕ_s) between VaR and scenario cost (Cost_s), are introduced to manage the risk as shown in Figure 4. If the Cost_s is less than VaR, ϕ_s should be enforced to zero. At a given confidence interval, there is a VaR, defined as a minimum value that probability of cost exceeding or equaling to this value is greater or equal to α. The above relationships can be modeled by the following constraints

$$\text{VaR} \geq 0 \tag{34}$$

$$\phi_s \geq \text{Cost}_s - \text{VaR}, \quad \phi_s \geq 0, \quad s \in S \tag{35}$$

The CVaR associated with α quantile is defined by the following constraint

$$\text{CVaR}(x,\alpha) = \frac{\sum_{s\in S} p_s \cdot \phi_s}{1-\alpha} + \text{VaR} \tag{36}$$

Thus, the CVaR management model is given below

$$\min E[Cost] = Cost^{capital} + \sum\nolimits_{s\in S} p_s Cost_s^{2stg} \tag{28}$$

$$\min\ \text{CVaR}(x,\alpha) = \frac{\sum_s p_s \cdot \varphi_s}{1-\alpha} + \text{VaR} \tag{37}$$

$$\text{s.t.}\ \ \varphi_s \geq \text{Cost}_s - \text{VaR}, \quad \varphi_s \geq 0, \quad s \in S \tag{38}$$

$$\text{VaR} \geq 0 \tag{39}$$

Constraints 1–27

Similar to the downside risk management model, a CVaR management model also has two objective functions: minimizing both the total expected cost (Eq. 28) and CVaR (Eq. 37) subjected to constraints 38, 39, and 1–27.

Solution Algorithm

Stochastic programming models, like the problem addressed in this work could be computationally very demanding because their model size increases exponentially as the number of scenarios increases. In particular, the deterministic equivalent of such problems might not be solved directly due to its potentially very large size. To circumvent these difficulties, a decomposition algorithm is proposed.

A popular method for solving large scale stochastic programming models is the L-shaped method proposed by Van slyke and Wets,[50] which takes advantage of the special decomposable structure of the two-stage stochastic programming model. Consider the following general form of the two-stage stochastic programming model ($P0$).

$$(P0) \qquad \min_{x,y_s} c^T x + \sum_{s\in S} p_s q_s^T y_s \tag{40}$$

$$s.t.\ \ Ax = b, \qquad x \geq 0 \tag{41}$$

$$W_s y_s = h_s - T_s x, \qquad y(w_s) \geq 0,\ s \in S \tag{42}$$

where x is the vector that stands for the first-stage decision variables, and y_s represents the second-stage decisions for each scenario s. The objective function in ($P0$) represents the objective function given in constraint 28. Constraint 41 stands for the constraints with first-stage variables that are constraints 1–7 and 20. Constraint 42 represents for the second-stage constraints that include 8–19 and 21–27. c and q_s are the vectors of coefficients for the first- and second-stage decisions of the objective function, A and b are parameter matrixes independent of the scenarios, whereas W_s, h_s, and T_s are parameter matrixes for each scenario $s \in S$.

The expanded form of the original two-stage stochastic programming model ($P0$) is given below. The model has a special "angular" form, which can be decomposed into a master problem and a number of scenario subproblems.

$$\begin{aligned} &\min_{x,y_s} c^T x + p_1 q_1^T y_1 + p_2 q_2^T y_s + \ldots + p_s q_s^T y_s \\ &s.t\ Ax = b, \quad x \geq 0 \qquad \text{master problem} \end{aligned} \tag{43}$$

$$\left.\begin{array}{llll} T_1 x + & W_1 y_1 & & = h_1 \\ T_2 x + & & W_2 y_2 & = h_2 \\ \vdots & & \ddots & = \vdots \\ T_s x + & & W_s y_s & = h_s \end{array}\right\} \text{Scenario subproblems}$$
$$x \geq 0\ y_1 \geq 0\ y_2 \geq 0,\ \ldots\ y_s \geq 0 \tag{44}$$

The basic idea of the standard L-shaped method is to first solve the master problem to obtain the values of first-stage decisions. Then by fixing the first-stage decisions from the previous step, we solve all the scenario subproblems that only include second-stage decisions.

If we define $Q_s(x)$ as the objective function value of each scenario subproblem s

$$\begin{aligned} Q_s(x) &= \min_{y_s} q_s^T y_s \\ s.t.\ W_s y_s &= h_s - T_s x,\ y(w_s) \geq 0 \end{aligned} \tag{45}$$

then the reformulation of ($P0$) is as follows

$$(P0) \qquad \min_x c^T x + \sum_{s \in S} p_s Q_s(x) s.t.\ Ax = b, \qquad x \geq 0 \tag{46}$$

To solve ($P0$), we can take advantage of the dual properties of Eq. 45 by introducing a new variable θ for $\sum_{s \in S} P_s Q_s(x)$, and iterate between the master problem ($P1$) and the scenario subproblem ($P2$).

The master problem ($P1$) is given by

$$\begin{aligned} &\min_x c^T x + \theta \\ (P1) \qquad &s.t.\ \theta \geq e^{\text{iter}} x + d^{\text{iter}} \qquad \text{iter} = 1 \ldots N \\ &Ax = b \qquad x \geq 0 \end{aligned} \tag{47}$$

whereas the subproblem (P2) for scenario s is given by

$$\begin{aligned} &\min_y q_s^T y_s \\ (P2) \qquad &s.t.\ W_s y_s = h_s - T_s x, y(w_s) \geq 0 \end{aligned} \tag{48}$$

where the inequalities in ($P1$) are the "cuts" that link the master problem and the scenario subproblems. e^{iter} and d^{iter} are coefficients for the Benders cut, and they are given by

$$e^{\text{iter}} = -\sum_{s \in S} p_s \pi_{\text{iter},s}^T T_s \tag{49}$$

$$d^{\text{iter}} = \sum_{s \in S} p_s \pi_{\text{iter},s}^T h_s \tag{50}$$

where π_s^T are the optimal dual vectors of constraint 48 in the subproblem ($P2$) for scenario s. At each iteration step, the standard L-shaped method only returns one cut to the master problem. To speed up the algorithm, we can decompose the variable θ by scenarios to return as many cuts as the number of scenarios in each iteration. In this way, the proposed approach provides stronger cuts to the master problem, thus it reduces the number of iterations required to solve the problem. The master problem is then given by ($P3$).

$$\begin{aligned} &\min_x c^T x + \sum_{s \in S} p_s \theta_s \\ (P3) \qquad &\text{s.t.}\ \ \theta_s \geq e_s^{\text{iter}} x + d_s^{\text{iter}} \qquad \text{iter} = 1 \ldots N \quad \forall s \in S \\ &Ax = b \qquad x \geq 0 \end{aligned} \tag{51}$$

where e_s^{iter} and d_s^{iter} are the coefficients of the cuts that link the master problem and each scenario subproblem, they are updated as follows

$$e_s^{\text{iter}} = -\pi_{\text{iter},s}^T T_s \tag{52}$$

$$d_s^{\text{iter}} = \pi_{\text{iter},s}^T h_s \tag{53}$$

The major steps of the multicut algorithm are given below:

Step 1: initialization: $LB = -\infty$, $UB = +\infty$, tolerance: Tol.

Step 2: set iter = 1

Step 3: at iteration iter, solve the master problem ($P3$) and store the first-stage variables.

Step 4: update the lower bound

Step 5: fix first-stage variables from the step 3 and solve each scenario subproblem.

Step 6: Update the upper bound

Step 7: If $UB - LB \leq Tol$, stop and retrieve the optimal value, otherwise retrieve the duals of the scenario subproblems and compute the coefficients of the optimality cuts Eqs. 52 and 53. Then set iter = iter + 1, go to step 3.

The algorithmic framework for multicut L-shaped method is given in Figure 5.

The Pareto-optimal set of solution that reveals the trade-offs between the economic performance and the financial risk metrics is obtained by applying ε-constraint method. This method is based on formulating an auxiliary model, which is obtained by transferring one of the objectives of the original problem to an additional constraint. This constraint imposes an upper limit on the value of the secondary objective. The new model is then solved for different values of the auxiliary parameter ε to generate the entire Pareto set of solutions. The proposed optimization approach is illustrated through four case studies of hydrocarbon biorefinery supply chains for the State of Illinois.

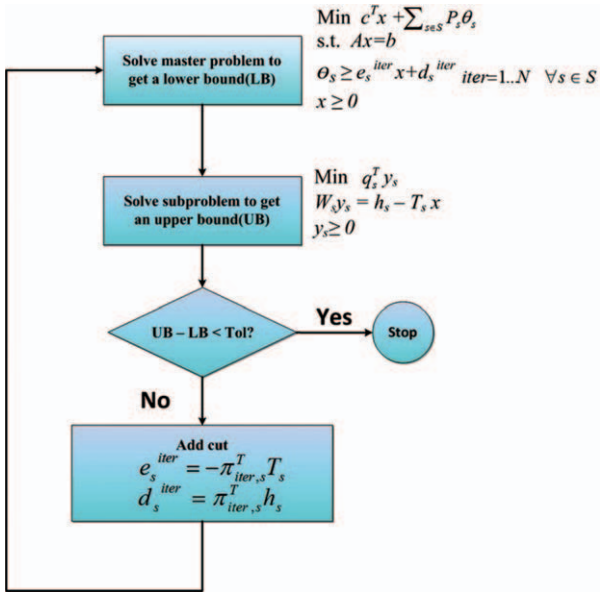

Figure 5. Algorithm for multicut L-shaped approach.

[Color figure can be viewed in the online issue, which is available at wileyonlinelibrary.com.]

County—Level Case Studies for the State of Illinois

To demonstrate the effectiveness of the proposed models, we present the results of four case studies for the State of Illinois. The computational studies were performed on a Dell Optiplex 790 Desktop with Intel(R) Core(TM) i5-2400, 3.10 GHz CPU, and 8 GB RAM. The MILP model was coded in GAMS 23.7[51] and solved with the solver CPLEX 12.

Input Data

Case Study 1: Deterministic Model. In the first case study, a deterministic model is adopted to minimize the total cost. We assume that supply and demand are both fixed, and 10% of current fuel usage in Illinois is met by the hydrocarbon biofuels.

The State of Illinois consists of 102 counties. Each county is considered as a potential harvesting site, a possible hydrocarbon biorefinery location, and a demand zone. Thus, the supply chain network in this case study has 102 harvesting sites, 102 hydrocarbon biorefinery location candidates, and 102 demand zones. We use Google Map to get the distance between counties. The cost data of transportation is obtained from Searcy et al.[52] and Mahmud and Flynn.[53]

In this case study, three major types of biomass are considered. They are agricultural residues (e.g., corn stover), energy crops (e.g., switchgrass), and wood residues (e.g., urban wood residues, primary mills and forest residues). The annual amount of available biomass is given in Table 1 from U.S. Department of Agriculture statistical data, and their spatial distributions are presented in Figure 6. The spatial data of biomass distribution used in this article is the same with those in You et al.[27] The influence of seasonality on biomass feedstock is estimated by considering 12 time periods in each year. Some agricultural residues are only available in some of the months. For Illinois, corn stovers are usually harvested from early September to the end of November. In addition, because of deterioration, all biomass collected could not be fully used. Deterioration rate of feedstock is estimated as 0.5% per month for on-site storage. The harvesting costs are obtained from Petrolia[54] and Eksioglu et al.[55]

Two types of hydrocarbon biofuels, diesel and gasoline, are produced and shipped to demand zones. Monthly demands of hydrocarbon biofuels in Illinois are obtained from U.S. Energy Information Administration (EIA) forecasts using time-series methods with Oracle Crystal Ball.[56] We assume that the demand of each specific county is proportional to its population that is obtained from the U.S. Census Bureau and listed in Table 1. The demands of diesel and gasoline have mild variation in different time periods which are shown in Figure 7.

In this case study, we consider two major conversion technologies: gasification followed by FT synthesis and fast pyrolysis followed hydroprocessing. The capacities for both of them have three levels: 1–50 MGY (million gallons per year), 50–100 MGY, and 100–200 MGY. Government incentives are taken into account in the annual total cost. It includes biorefinery construction incentives and volumetric incentives for hydrocarbon biofuels production.

Case Study 2: Stochastic Programming Model with Four Scenarios. In the rest of the case studies, types of hydrocarbon biofuels, conversion technologies, and production capacity levels are considered the same as the first case study. In the first case study, supply and demand are fixed values. Whereas in this case study, we consider four scenarios with different supply and demand, which are given in Table 2. Each scenario has the same probability of 0.25. S and D represent the deterministic amount of supply and demand for each county at each time period, respectively. σ is standard deviation of the demand for each county at each time period, which is also obtained from time-series forecasting with Oracle Crystal Ball[56] based on the EIA data. $1.5S$ shows that the supply in Scenario 1 is 1.5 times the amount of biomass supply in each county at each time period of the deterministic one. $D + 3\sigma$ means that the demand in Scenario 3 is 3 standard deviations from the demand D on the larger side for each county at each time period. Similarly, $D - 3\sigma$ is 3 standard deviations from D on the smaller side. The average values of supplies and demands in four scenarios are equal to S and D. In other words, unlike the deterministic model, the supplies and demands in four scenarios fluctuate around S and D. The biomass supply may increase because of suitable weather or decrease because of unfavorable conditions; while demand may rise for increasing desire of clean energy or reduce as a result of economic recession. The input data of stochastic programming models reflect the real situation more effectively.

Case Study 3: Stochastic Programming Model with 100 Scenarios and Risk Management. In this case study, we consider 100 scenarios. Biomass supply and hydrocarbon biofuels demand are uncertain and both of them follow normal distribution, whose mean values are the same as the supply and demand of the deterministic case study. The deviations are derived from historical record. The 100 scenarios represent 100 possible realizations of uncertain parameters. Monte Carlo sampling method is used to generate scenarios as follows

$$\mathrm{BA}_{b,i,t,s} = \mathrm{Max}\{0,\ \mathcal{N}(\mathrm{BA}_{b,i,t}, \mathrm{BA}_{b,i,t}/3)\} \tag{54}$$

$$\mathrm{DEM}_{k,p,t,s} = \mathrm{Max}\{0,\ \mathcal{N}(\mathrm{DEM}_{p,k,t}, \sigma_{--}\mathrm{DEM}_{p,k,t})\} \tag{55}$$

where $\mathrm{BA}_{b,i,t}$ is the mean of the amount of biomass b available in harvesting site i at time period t, and $\mathrm{DEM}_{p,k,t}$ is the mean of demand of hydrocarbon biofuel p in demand zone k at time

Table 1. Biomass Resource and Population of Each County in Illinois

FIPS	County	Crop Residue (t/year)	Energy Crops (t/year)	Wood Residues (t/year)	Population
17,085	Adams	256,393	95,702	15,442	68,277
17,177	Alexander	28,281	12,356	6923	9590
17,201	Bond	103,029	70,462	4770	17,633
17,097	Boone	109,989	5089	5625	41,786
17,111	Brown	78,013	77,184	10,400	6950
17,007	Bureau	457,925	44,171	7429	35,503
17,141	Calhoun	28,933	50,246	10,733	5084
17,015	Carroll	232,260	52,515	3466	16,674
17,031	Cass	149,716	69,525	19,954	13,695
17,089	Champaign	530,993	53,512	19,743	179,669
17,037	Christian	356,408	44,089	8131	35,372
17,043	Clark	186,746	33,927	5397	17,008
17,195	Clay	87,579	76,912	33,839	14,560
17,103	Clinton	150,966	37,596	32,655	35,535
17,161	Coles	201,385	25,310	9672	53,196
17,197	Cook	9266	10	606,890	5,376,741
17,093	Crawford	124,770	58,253	3709	20,452
17,099	Cumberland	123,588	40,165	5342	11,253
17,011	De Witt	185,852	16,950	2043	16,798
17,073	DeKalb	322,151	20,161	18,158	88,969
17,063	Douglas	232,764	23,596	4688	19,922
17,131	DuPage	7305	0	107,435	904,161
17,155	Edgar	291,367	28,239	2285	19,704
17,091	Edwards	47,139	38,695	1550	6971
17,175	Effingham	137,978	50,844	34,858	34,264
17,095	Fayette	153,509	86,084	33,381	21,802
17,123	Ford	281,914	34,716	1786	14,241
17,105	Franklin	47,335	131,415	37,231	39,018
17,071	Fulton	264,261	46,822	45,290	38,250
17,187	Gallatin	85,285	24,363	4096	6445
17,075	Greene	213,534	70,331	5685	14,761
17,053	Grundy	170,393	10,652	4097	37,535
17,143	Hamilton	80,647	176,653	9510	8621
17,203	Hancock	314,904	105,538	26,029	20,121
17,113	Hardin	3982	13,194	3859	4800
17,179	Henderson	170,516	8910	2692	8213
17,057	Henry	439,901	80,412	9630	51,020
17,067	Roquois	632,935	86,149	18,324	31,334
17,109	Jackson	62,571	66,178	13,466	59,612
17,183	Jasper	148,258	47,459	11,484	10,117
17,125	Jefferson	68,589	176,147	13,238	40,045
17,019	Jersey	101,379	30,329	6121	21,668
17,107	Jo Daviess	128,533	149,045	19,514	22,289
17,169	Johnson	12,703	103,458	27,905	12,878
17,039	Kane	135,678	929	51,555	404,119
17,147	Kankakee	287,993	13,156	12,524	103,833
17,001	Kendall	116,130	3260	12,187	54,544
17,129	Knox	322,106	65,835	21,803	55,836
17,017	La Salle	487,821	38,978	12,467	111,509
17,009	Lake	16,183	0	76,129	644,356
17,115	Lawrence	104,237	38,314	13,677	15,452
17,167	Lee	383,320	19,551	3934	36,062
17,045	Livingston	554,660	55,297	4982	39,678
17,041	Logan	358,837	52,151	5894	31,183
17,137	Macon	264,794	14,723	12,956	114,706
17,149	Macoupin	328,871	71,431	49,768	49,019
17,021	Madison	206,142	19,704	40,053	258,941
17,139	Marion	112,770	173,028	35,089	41,691
17,171	Marshall	170,689	9792	2272	13,180
17,029	Mason	206,486	55,575	23,455	16,038
17,173	Massac	27,807	62,074	22,482	15,161
17,135	McDonough	286,329	37,960	12,027	32,913
17,117	McHenry	130,706	9611	37,232	260,077
17,061	McLean	640,168	55,079	17,195	150,433
17,023	Menard	156,021	35,271	1667	12,486
17,013	Mercer	269,911	72,285	3148	16,957
17,035	Monroe	88,501	23,759	20,010	27,619
17,083	Montgomery	278,150	66,352	25,759	30,652
17,051	Morgan	266,676	38,505	13,577	36,616
17,049	Moultrie	152,398	10,625	4000	14,287
17,033	Ogle	312,484	61,034	10,636	51,032
17,079	Peoria	215,911	21,408	21,753	183,433

Table 1. (Continued)

FIPS	County	Crop Residue (t/year)	Energy Crops (t/year)	Wood Residues (t/year)	Population
17,005	Perry	61,622	51,084	6605	23,094
17,119	Piatt	231,675	14,152	1756	16,365
17,025	Pike	232,057	194,823	27,094	17,384
17,101	Pope	8025	58,655	12,338	4413
17,159	Pulaski	35,468	55,449	4250	7348
17,121	Putnam	61,956	17,886	1303	6086
17,027	Randolph	99,209	52,118	22,213	33,893
17,163	Richland	103,535	38,619	9937	16,149
17,191	Rock Island	140,432	38,750	21,701	149,374
17,047	Saline	45,045	49,070	16,407	26,733
17,185	Sangamon	413,194	62,106	23,349	188,951
17,133	Schuyler	122,711	87,243	29,192	7189
17,189	Scott	92,286	30,579	2517	5537
17,081	Shelby	262,610	71,654	10,724	22,893
17,193	St. Clair	155,565	15,632	40,229	256,082
17,065	Stark	177,849	14,435	681	6332
17,157	Stephenson	232,457	40,597	5793	48,979
17,145	Tazewell	276,646	42,701	14,978	128,485
17,055	Union	26,645	111,204	18,319	18,293
17,077	Vermilion	421,013	36,311	9695	83,919
17,059	Wabash	67,370	21,990	7972	12,937
17,165	Warren	296,053	13,128	2260	18,735
17,199	Washington	143,426	38,788	7884	15,148
17,087	Wayne	122,597	266,531	26,661	17,151
17,181	White	106,138	65,351	41,548	15,371
17,151	Whiteside	353,271	74,060	7229	60,653
17,069	Will	186,563	8910	62,079	502,266
17,127	Williamson	11,149	59,461	14,670	61,296
17,003	Winnebago	120,942	27,683	34,144	278,418
17,153	Woodford	281,221	32,016	4361	35,469

period t. $\sigma\_DEM_{p,k,t}$ and $BA_{b,i,t}/3$ are standard deviations of demand and supply, respectively. We add "Max" to guarantee that supply and demand in all scenarios are non-negative.

We also introduce risk management formulations to reduce economic losses due to unfavorable scenarios and simultaneously improve the economic performance measure objective. Thus, we have a multiobjective optimization problem whose optimal solution yields a Pareto-optimal curve. Two types of risk management models are adopted in this case study: CVaR and downside risk.

Case Study 4: Stochastic Programming Model with 1000 Scenarios. Through statistical approach, 1000 scenarios are required to achieve a reasonable confidence interval.[40] All the scenarios are generated using the same method as those in case study 3. Because of the large size of the problem, it creates huge computational burden to solve it directly. In this article, multicut L-shaped decomposition algorithm is implemented to obtain the optimal solution. The computational performance comparison between multicut L-shaped and the standard L-shaped decomposition approaches in terms of CPU times and the number of iterations are discussed.

Results of Deterministic and Stochastic Programming Models

The sizes of the resulting stochastic programming problems in case studies 2, 3, and 4 are very large, compared to the size of deterministic model, which can be viewed in Table 3. When the scenarios increase from 4 to 1000, continuous variables and constraints increase exponentially. As the number of scenarios increase, the solutions become closer to the realistic situation.

However, the larger size of the problem leads to more computational challenge. By implementing the multicut L-shaped method, we reduce the CPU times and the number of iterations required to get the optimal solution with reasonable optimality gap.

Results for Deterministic Model. The minimum cost solution of the deterministic model leads to the optimal total cost of \$2,699,311,660, and the corresponding unit cost of hydrocarbon biofuels product in terms of GEG is \$4.00/GEG. The optimal locations of hydrocarbon biorefinery, plant capacities, and selected conversion technologies are given in Figure 8. The background of Figure 8a is the service zones of hydrocarbon biorefineries; counties in the same color means their biofuel demands are satisfied by one hydrocarbon biorefinery. If demand of a county is provided by multiple plants, it is regarded as a service zone of its main provider. Figure 8b is the distribution of hydrocarbon biorefineries on the background of biomass supply zones. Counties in identical color transport biomass to the same plant. Similarly, if a county ships biomass to several plants, it is assigned to the plant that receives the most of feedstock from that county. Counties in gray do not supply feedstock to any plant.

Figure 8 shows that total 11 hydrocarbon biorefineries are constructed in 11 counties, and five of them are in the north part of Illinois, another five are located in central Illinois, and the one left is built in southern Illinois. From Figures 8a and b, one can see that one hydrocarbon biorefinery with a large capacity of 76 MGY is built in Cook County, but it can only meet its local demand. This is the result of high local demands of hydrocarbon biofuels due to high population density. The plant in La Salle County has the largest capacity of 169 MGY with dense population; it provides biofuels to six counties. Iroquois County and Livingston County also have relatively large capacities for the same reason. However, some other hydrocarbon biorefineries (e.g., biorefineries in Henry County and Sangamon County) serve more

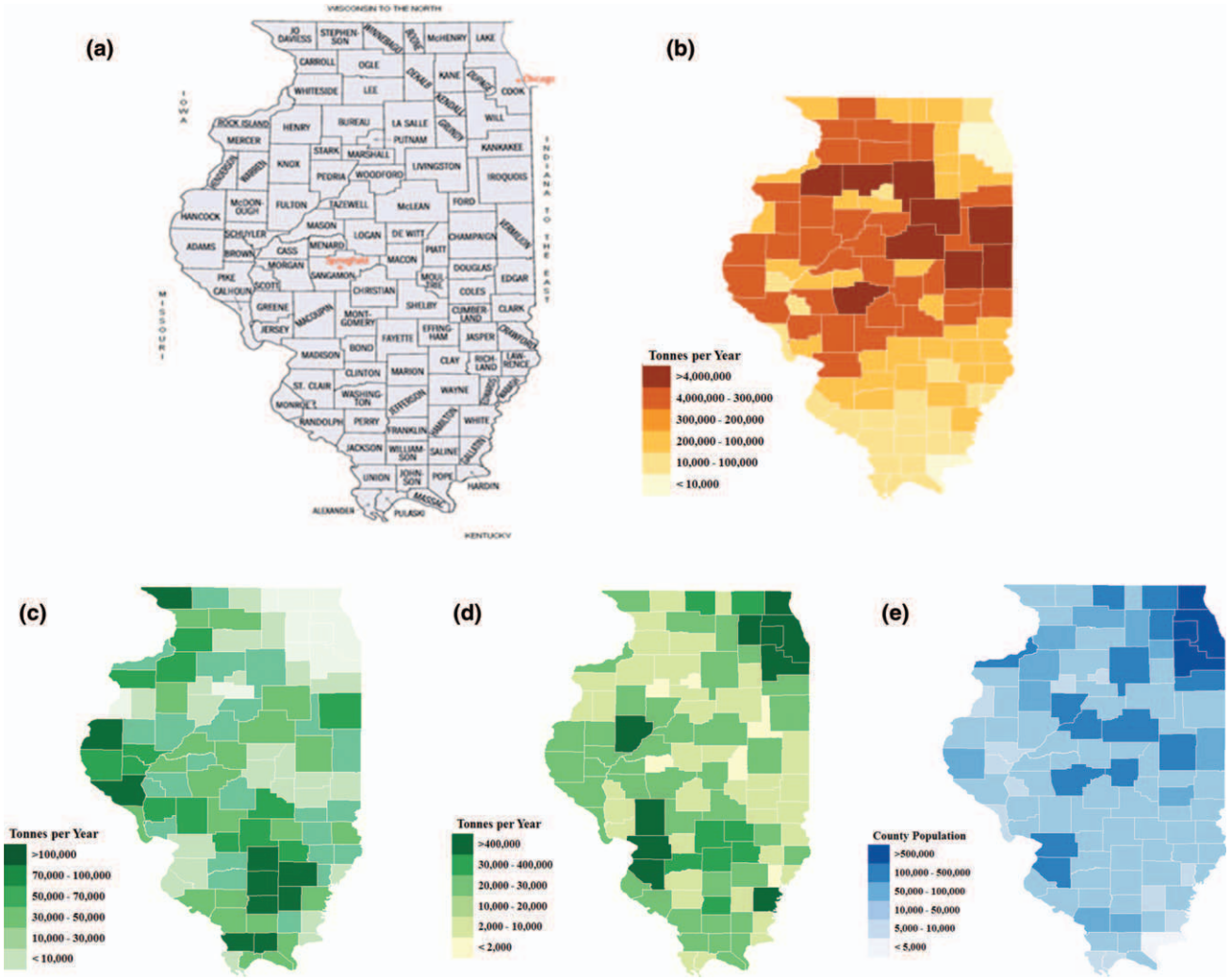

Figure 6. Spatial distributions of cellulosic biomass resources and the population density of the State of Illinois.

(a) County map of Illinois. (b) Spatial distribution of crop residues in Illinois. (c) Spatial distribution of energy crops in Illinois. (d) Spatial distribution of wood residues in Illinois. (e) Population density distribution. [Color figure can be viewed in the online issue, which is available at wileyonlinelibrary.com.]

counties with smaller capacities because of low demands. In general, hydrocarbon biorefineries are built in counties with both high demand and abundant biomass to reduce transportation distance, and thus decreases transportation costs.

Figure 8b shows that not all counties are involved in supplying biomass to hydrocarbon biorefineries. A biorefinery plant is usually supplied by nearby counties. For instance, Wayne County takes advantage of biomass coming from a local harvesting site and seven adjacent counties. Such an assignment reduces the average transportation distance. With respect to technology selection, the plant in La Salle County adopts gasification while the rest of biorefineries choose fast pyrolysis. The main reason is that fast pyrolysis has a relatively high yield of gasoline, which can be demonstrated in Table 4, and local demands of gasoline are higher than diesel. Another reason is that most agricultural residues in Illinois are corn stovers. Fast pyrolysis followed by hydroprocessing is more economical and suitable for producing

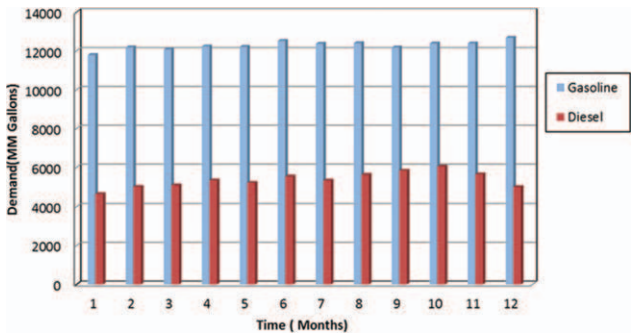

Figure 7. Monthly demands of gasoline and diesel in Illinois.

[Color figure can be viewed in the online issue, which is available at wileyonlinelibrary.com.]

Table 2. Supply and Demand of Deterministic and Stochastic Programming Models

	Supply	Demand
Deterministic model	S	D
Scenario 1	$1.5S$	D
Scenario 2	$0.5S$	D
Scenario 3	S	$D + 3\sigma$
Scenario 4	S	$\text{Max}\{0, D - 3\sigma\}$

Table 3. Model Sizes of the Four Case Studies

	Deterministic	Four scenarios	100 scenarios	1000 scenarios
Binary variables	408	408	408	408
Continuous variables	652,296	2,605,806	65,118,126	651,171,126
Constraints	30,708	118,842	2,939,130	29,379,330

hydrocarbon biofuels from corn stovers than gasification technology.[4,5,27]

Results for Stochastic Programming Model with Four Scenarios. The total costs of the stochastic solutions are given in Figure 9. The expected cost of stochastic solution is \$5,711,840,000. The total cost of Scenario 4 is \$1,855,112,000 that is 31% lower than deterministic solution, whereas total cost of scenarios 1, 2, and 3 are \$2,722,336,000, \$9,970,945,000, and \$1,855,112,000, respectively. Scenario 4 has the lowest cost because of the lowest demand. On the contrary, high demand leads to a high cost, as the situation in Scenario 3. Moreover, reduced supply also contributes to a high cost, as the situation in Scenario 2. These results reflect that either variation of supply or demand causes significant changes of the total cost. The components of total cost also vary a lot in the four scenarios. Transportation cost is a typical example sensitive to the fluctuation of supply and demand. In Scenario 2 with low supply and Scenario 3 with high demand, transportation accounts for a considerable percentage of the total cost; in Scenario 1 with high supply and Scenario 4 with low demand, transportation cost is quite small compared to other cost. This is because when biomass supply decreases or biofuel demand increases, local biomass may not satisfy demands of the local biorefineries. Thus, shipments of biomass from other counties are required. The total costs of scenarios 1, 2, and 3 are higher than the total cost of the deterministic solution, which is \$2,699,311,660. When demand grows significantly (e.g., Scenario 3) or supply decreases (e.g., Scenario 2), the biorefineries fail to meet local demands with a uniform cost given by deterministic model. Even in Scenario 1 that has higher supply but same demand with deterministic case, the total cost is slightly higher. Because the additional biomass supply is collected, capital and O&M cost become higher.

Figure 10 presents the comparison of total biomass and biofuel inventory levels of hydrocarbon biorefinery among the four scenarios. Figure 10a indicates a remarkable seasonality in the inventory profile. The total inventory level reaches its peak in November. This trend is because of seasonality of corn stovers harvest, which is the main biomass resources. Limited by production capacities of biorefineries, biomass harvested cannot be fully used to produce hydrocarbon biofuels, thus some unused biomass resources are stored and ready to be used in the next time periods. Because of the lowest biomass supply, Scenario 2 has the lowest inventory. Scenario 3 has the maximum inventory level because of its highest local demands of hydrocarbon biofuels.

Similar to the biomass inventory levels trend shown in Figure 10a, the inventory levels of the hydrocarbon biofuels shown in Figures 10b and c also reflect strong seasonality. This trend shows the direct relationship between the biomass inventory and hydrocarbon biofuel inventories. Another factor affecting the hydrocarbon biofuels inventory level is the demand. In Figures 10b and c, Scenario 3 always has the lowest hydrocarbon biofuel inventory level, because the demand of hydrocarbon biofuels is so high that all products are sold out. On the contrary, in Scenario 4, it is not necessary to hold a considerable inventory level as the demand of hydrocarbon biofuels is quite low.

From Figure 10, we can conclude that both feedstock and product inventory levels are subjected to variation of supply

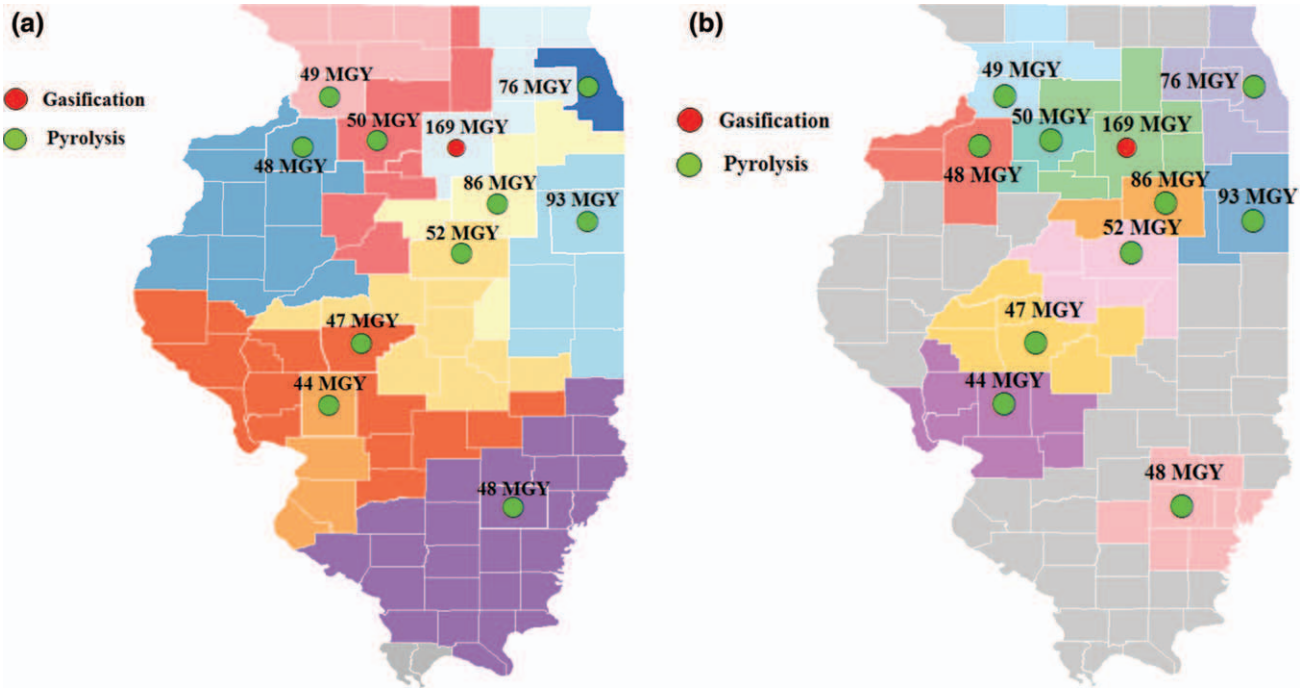

Figure 8. Optimal plant locations, capacities, and selection of technology in deterministic case.

(a) Optimal location of plants with background of service zone map. (b) Optimal location of plants with background of supply zone map. [Color figure can be viewed in the online issue, which is available at wileyonlinelibrary.com.]

Table 4. Capacities, Total Capital Investments and Yields of Reference Plants

Technology	Capacity	Capital Investment	Yields
Biomass gasification + FT synthesis	35.0 MM GEG/year	$341.00 MM	21.64 gal of gasoline/ton of biomass; 44.18 gal of diesel/ ton of biomass
Biomass pyrolysis +hydroprocessing	35.4 MM GEG/year	$287.40 MM	41.01 gal of gasoline / ton of biomass; 9.48 gal of diesel/ton of biomass

and demand. Stochastic programming takes this into account at the design stage and accordingly adjusts its solution that will be more robust than the one given by the deterministic model.

The optimal locations of hydrocarbon biorefineries in the stochastic solution are given in Figures 11 and 12. The background of Figure 11 is the demand zone map and the one for Figure 11 is supply zone map. As mentioned in the first case study, when a county ships biomass to multiple plants or a demand zone is served by several plants, we only consider the main biomass receiver and main biofuel provider, respectively. Compared to hydrocarbon biorefinery sites of the deterministic solution, the results of stochastic solutions differ in a way to accommodate the variation in supply and demand. Plants in Bureau County with a capacity of 50 MGY and in Iroquois County with a capacity of 93 MGY are not included in the stochastic solution while they are constructed in the deterministic case. Instead, a hydrocarbon biorefinery with a capacity of 90 MGY is constructed in Pike County and another one with 88 MGY is constructed in Wayne County. The rest of the plants are constructed in the same counties as the deterministic solution, but with distinct capacities, service areas, and supply zones. These adjustments are made due to the changes of supply and demand of the four scenarios. When the supply of biomass fluctuates, plants of some counties in the deterministic solution may not be able to collect enough biomass while some other counties have high storage level. Similarly, when demand of hydrocarbon biofuels goes up and down, hydrocarbon biorefineries in some counties assigned in the deterministic solution may fail to meet local or adjacent demands while some others do not fully use their production capacities.

Figure 11 shows the service zone maps of scenarios 1 and 2. Although, the demands in the two scenarios are the same as the deterministic case, the assignments of service zones are adjusted because of the variation in supply. For instance, Livingston County is a county where a plant is installed in both deterministic and stochastic solutions. It serves four counties in the deterministic solution. The increased supplies of biomass in Livingston County in Scenario 1 enable the

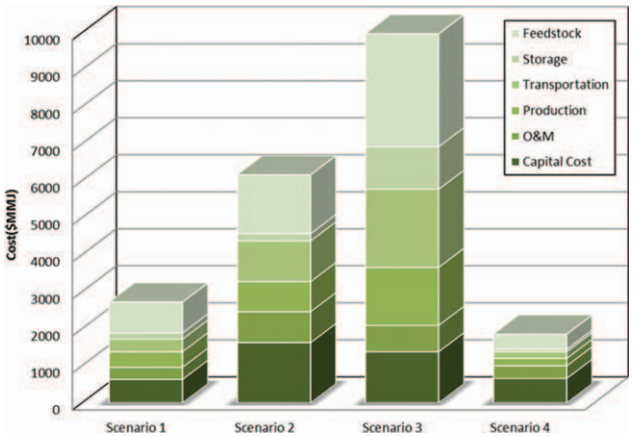

Figure 9. Components of total costs of stochastic solutions.

[Color figure can be viewed in the online issue, which is available at wileyonlinelibrary.com.]

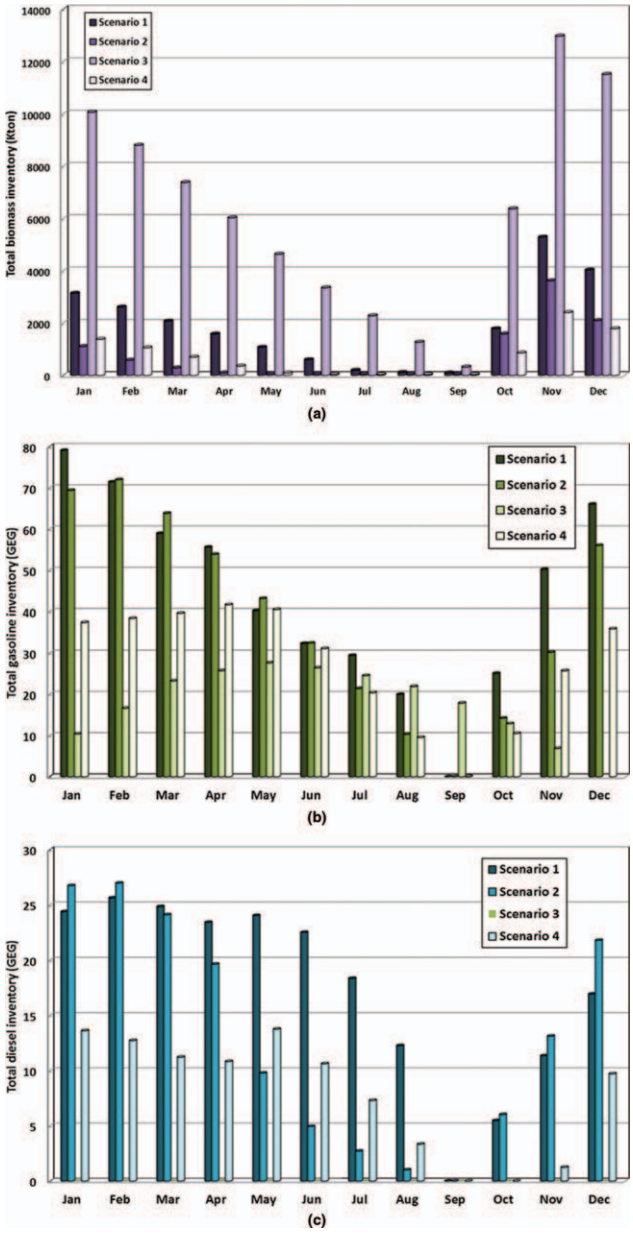

Figure 10. Total biomass/biofuel inventory levels in a year in four scenarios.

(a) Total biomass inventory in a year in four scenarios. (b) Total gasoline inventory in a year in four scenarios. (c) Total diesel inventory in a year in four scenarios. [Color figure can be viewed in the online issue, which is available at wileyonlinelibrary.com.]

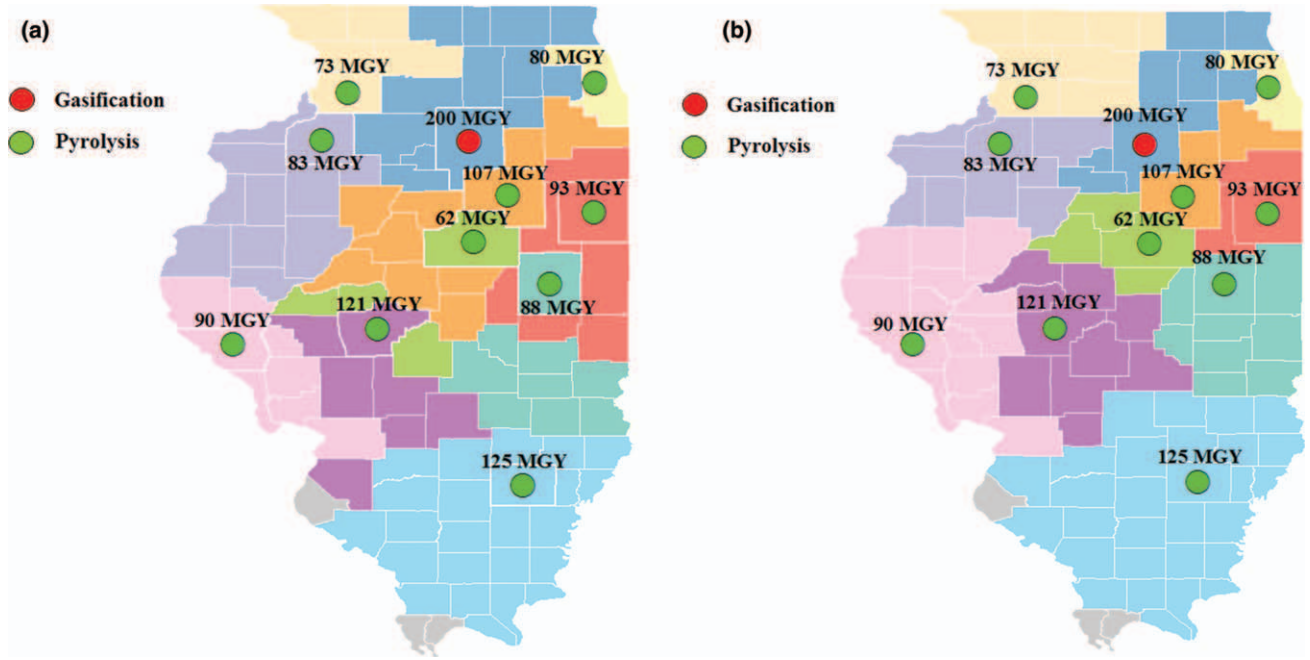

Figure 11. Optimal plant locations, capacities, selection of technology in scenarios 1 and 2.

(a) Results in Scenario 1. Background is a map for the serving areas of gasification and fast pyrolysis. (b) Results in Scenario 2. Background is a map for the serving areas of gasification and fast pyrolysis. [Color figure can be viewed in the online issue, which is available at wileyonlinelibrary.com.]

plant to produce more hydrocarbon biofuels and serve 10 counties. When the supply shrinks like in Scenario 2, the biorefinery in Livingston County can only satisfy demands of biofuels in three counties, as less biomass leads to less production. However, high supply does not guarantee that each hydrocarbon biorefinery can provide biofuels to more counties. Wayne County is a typical example. When the supply increases in Scenario 1, the number of counties whose local demands of biofuels are met by the biorefinery in Wayne County is reduced from 26 in the deterministic solution to 24 in the stochastic one. The service zones of Wayne County expand when the supply reduces by half. These changes are made to reduce the total cost when the supply increased by 50% compared to the deterministic case. The difference between Figures 11a and b reflects the impacts of uncertainty in feedstock supply and hydrocarbon biofuels demand.

Figures 12a–d show the assignments of supply zones for the four scenarios. Compared to supply zone map of the deterministic solution, Figure 12a shows that hydrocarbon biorefineries in Scenario 1 are supplied by fewer counties as a result of higher local biomass supply. As shown in Figure 12d, hydrocarbon biorefineries in Scenario 4 also have reduced the number of biomass suppliers. The reason for this situation is the reduced demands of hydrocarbon biofuels. On the contrary, when the supply decreases in Scenario 2 or the demand increases in Scenario 3, there are more harvesting sites involved in supplying biomass to hydrocarbon biorefineries. These are situations shown in Figures 12b and c. In the central Illinois shown in Figures 12b and c, we noticed a supply area without hydrocarbon biorefinery plant. This is because the counties in this area supply to a biorefinery that does not use local biomass. Thus, the county where this biorefinery is built is marked as the color different from its biomass supply area, leading to the supply area without any biorefinery. In these two scenarios, this assignment seems not economical for this particular biorefinery. However, stochastic programming model is looking for an optimal solution on average for all scenarios and, thus, such a solution can perform well under uncertainty, the solution which is better for those two scenarios may not be economical for all other scenarios.

When supply and demand fluctuate, the optimal deterministic solution of some variables can not hold all the constraints, which leads to an infeasible situation. To make a reasonable comparison between the deterministic case and the stochastic programming case, we fixed first-stage decision variables as that of the deterministic solution and solved the second-stage decisions of the four scenarios independently. Figure 13 shows components of biomass suppliers of Cook County in stochastic and deterministic solution. Cook is one of the counties where a biorefinery is built. The main biomass supplier is Cook itself. Taking advantage of local biomass can save transportation cost.

As biorefinery in Cook has a larger capacity in stochastic solution than that in the deterministic solution, the total amount of biomass shipped to Cook is expected to increase in stochastic scenarios. This is true for scenarios 1 and 4. However, Scenario 2, with less biomass supply in both cases, has the same amount of biomass transportation because limited biomass supply does not allow the biorefinery to produce at its capacity. An interesting phenomenon is that in Scenario 3, which has high demand and normal supply, the amount of biomass shipped to Cook in the stochastic case is less than the one in the deterministic case. Amount of local biomass and biomass shipped from DuPage is the same in both deterministic and stochastic solutions, but less biomass is shipped from the other counties to Cook in the stochastic solution than it is in deterministic case. From this, one can observe that for given hydrocarbon

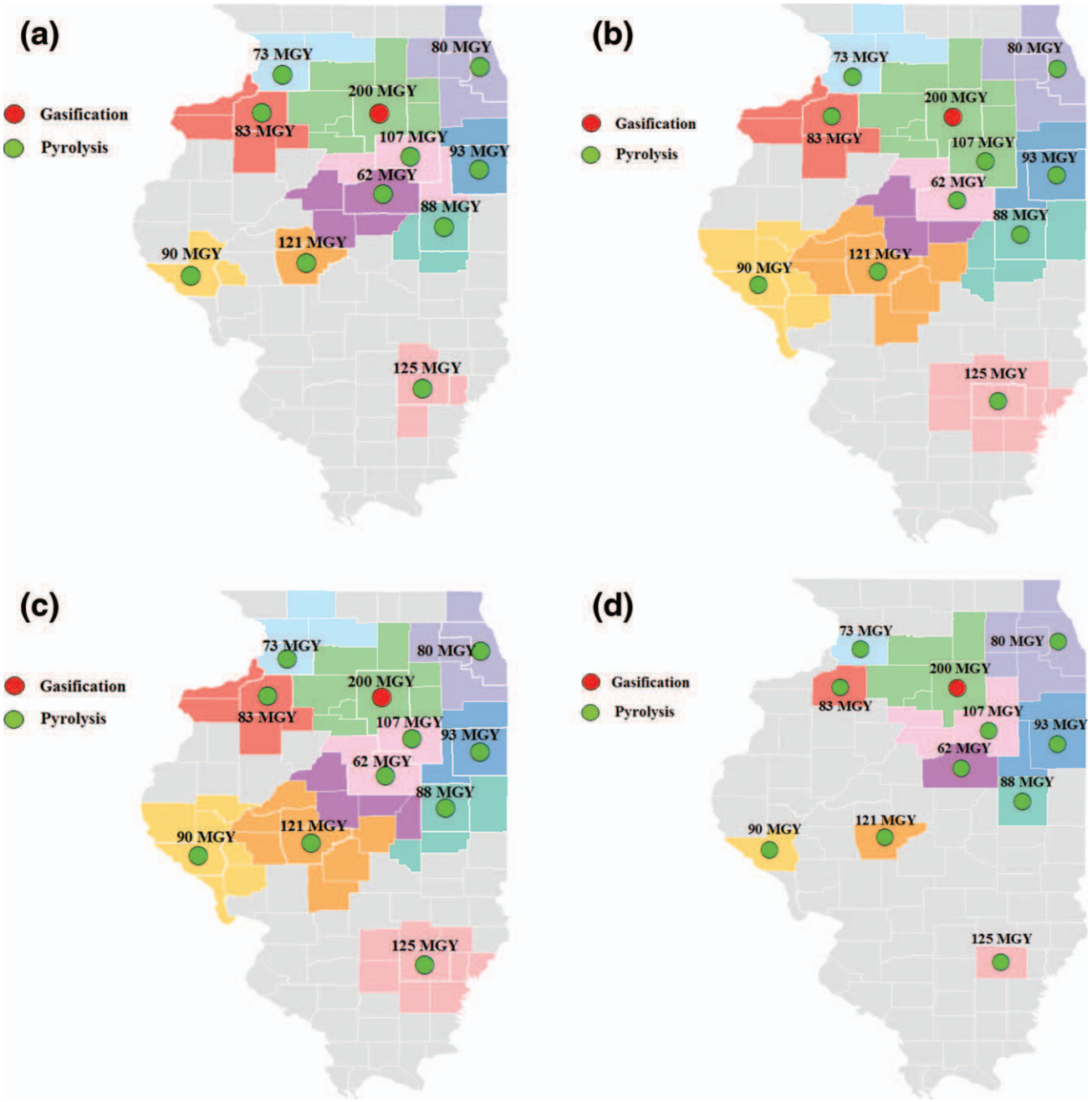

Figure 12. Optimal plant locations, capacities, and selection of technologies in four scenarios.

(a) Results in Scenario 1. Background is a map for biomass supply areas for each plant. (b) Results in Scenario 2. Background is a map for biomass supply areas for each plant. (c) Results in Scenario 3. Background is a map for biomass supply areas for each plant. (d) Results in Scenario 4. Background is a map for biomass supply areas for each plant. [Color figure can be viewed in the online issue, which is available at wileyonlinelibrary.com.]

biofuel demand and biomass supply, the stochastic and deterministic models have different biomass assignments.

Next, we compare transportation flows of diesel and gasoline of Cook County as shown in Figures 14 and 15. The total amount of diesel in *y*-axis of Figure 14 represents the demands of diesel hydrocarbon biorefinery in Cook County for each scenario, which is the same for both stochastic and deterministic cases. As shown in Figure 14, components of diesel demands met in Cook County in the stochastic solution are different from the deterministic one. For example, the diesel shipped from La Salle in stochastic Scenario 1 is less than that in deterministic Scenario 1 on the condition that they have the same demands and supplies. For scenarios 2 and 3 in both deterministic and stochastic cases, local demands are not fully met. Result of Scenario 2 indicates that when the biomass supply decreases to a certain level, the demand of diesel may not be satisfied. Whereas for Scenario 3, demand is not met as it raises a lot. When the demand of diesel increases too much, the plants fail to satisfy the demand in the optimal solution. Note that total unmet demands in deterministic cases are larger than that in stochastic one; we can conclude that stochastic model has a better performance under supply and demand uncertainty.

We have a similar result for gasoline, which is shown in Figure 15. As there is a hydrocarbon biorefinery built in Cook County, local production satisfies part of local demand.

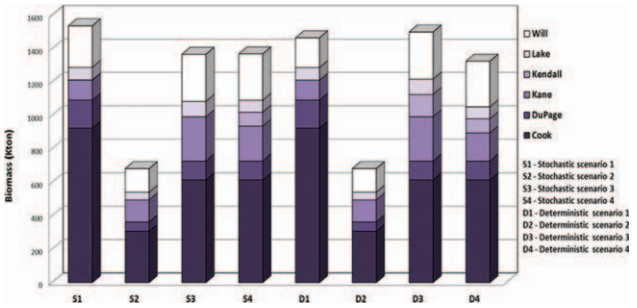

Figure 13. Components of biomass supplying to Cook in a year.

[Color figure can be viewed in the online issue, which is available at wileyonlinelibrary.com.]

Scenario 3 in both deterministic and stochastic cases has the highest demand, thus the demand is not met with 100% as the situation of diesel in the same scenario. The advantage of stochastic model is more obvious here, because the total amount of unmet demand in the stochastic solution is much smaller than that of the deterministic solution.

According to all results mentioned above, stochastic approach presents more realistic solutions to problems subjected to uncertainties of the design parameters. The deterministic approach does not consider the variability of parameters such as demand and supply uncertainty due to the variation in seasonality, weather conditions, economic situations, and so on. Therefore, it is unwise for decision makers to apply one deterministic solution to all possible variations. So, stochastic approach is advantageous to handle effects of uncertainties.

Results for Stochastic Programing Model with 100 Scenarios. For this case of 100 scenarios, two bicriterion stochastic MILP problems are considered. The results of minimizing expected annualized cost versus minimizing downside risk, and minimizing expected annualized cost versus minimizing CVaR, are discussed.

Results for Stochastic Programming Model with Economic Objective Case study with sample size of 100 scenarios is solved and the solutions of minimum expected annual cost are presented in Figure 16. The minimum total expected annualized cost is $2822.565 million (MM). The margin of error at 95% confidence interval is $15.595 MM that is a relatively small number compared to the total expected annualized cost. The optimal location of hydrocarbon biorefineries is shown in Figure 20.

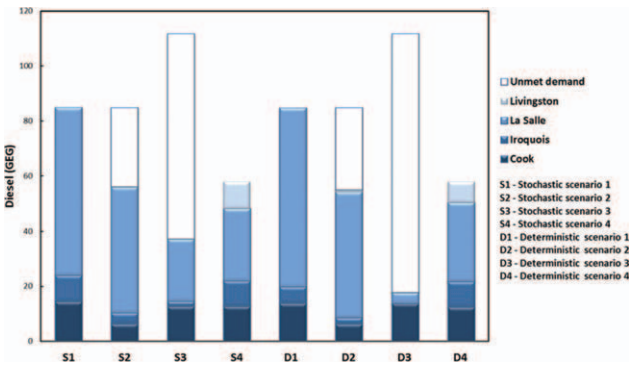

Figure 14. Components of diesel demand met in Cook.

[Color figure can be viewed in the online issue, which is available at wileyonlinelibrary.com.]

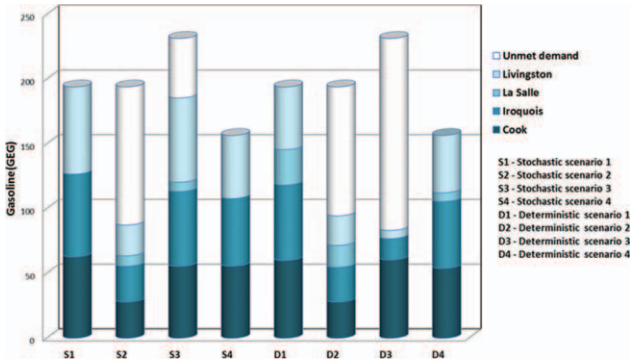

Figure 15. Components of gasoline demand met in Cook.

[Color figure can be viewed in the online issue, which is available at wileyonlinelibrary.com.]

Results for Downside Risk Management. Minimum downside risk solutions that consider target value Ω as $2900 MM together with minimum expected annualized cost solutions are presented in Figure 17. For minimum downside risk solution, the total expected annual cost rises to $2906.753 MM compared to $2822.565 MM of the minimum expected cost solution. But the risk in high-cost area has been effectively reduced. However, in this solution, the low-cost scenarios are pushed toward the target value $2900 MM. Although the risk in high-cost area (>$2900 MM) is decreased, the probability of obtaining low cost (<$2900 MM), in other words favorable scenarios, decreased significantly. If we desire a better solution, a new target value needs to be set. This result indicates that downside risk management highly depends on the value of Ω. It is tricky to find such a value of Ω that will lead to improvement because there is no established conventional way of choosing Ω.

Results for Managing CVaR. The solutions of minimum CVaR together with the minimum expected annual cost are given in Figure 18. We need to know about the cost corresponding to 90% α quantile. This figure shows that the cost corresponding to 90% decreases to $2889 MM after CVaR management compared to $2904 MM without CVaR management. For CVaR solution, the probability that the cost is

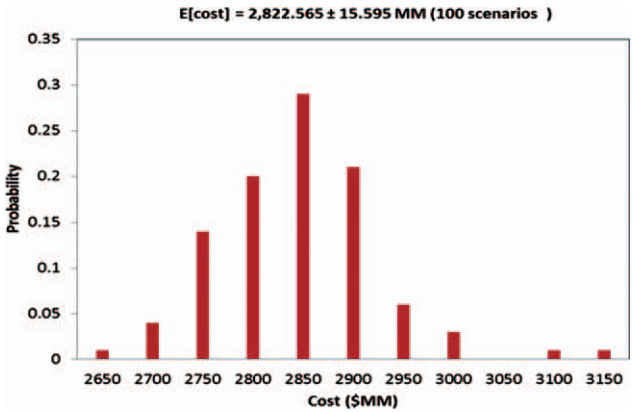

Figure 16. Histogram of the results for stochastic programming model with 100 scenarios.

[Color figure can be viewed in the online issue, which is available at wileyonlinelibrary.com.]

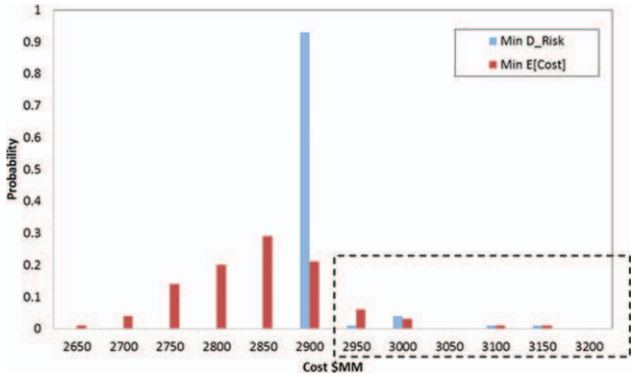

Figure 17. Comparison of the cost distribution after and before downside risk management (target value at $2900 MM).

[Color figure can be viewed in the online issue, which is available at wileyonlinelibrary.com.]

lower or equal to $2889 MM is 90%, whereas the probability that the cost lower or equal $2904 MM is also 90% in the solution of minimizing total expected annual cost. The risk in the latter one is higher, although its expected cost is lower.

Compared to downside risk management, CVaR does not depend on target value Ω. In addition, the probability of the cost below $2900 MM does not decrease considerably as it does in downside risk management. When CVaR is reduced, the chance of low-cost scenarios (<$2900 MM) is still very high. In this specific case study, CVaR is more convenient and effective.

As a bicriterion optimization problem, all the optimal solutions form a Pareto curve (Pareto frontiers). The Pareto curve obtained considering the expected annual cost and CVaR as objective functions is given in Figure 19. Solutions above the Pareto frontiers are feasible solutions, but any of these solutions does not perform better than the Pareto frontier; solutions below the curve are infeasible. In this figure, one can observe the optimal trade-off between the CVaR and the total expected annual cost. Designs in Points A and C stand for the extreme designs. The total expected annual

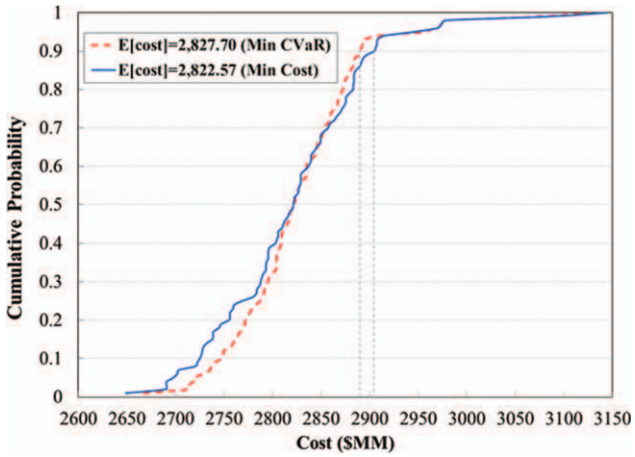

Figure 18. Comparison of cumulative probability cost distribution before and after managing CVaR.

[Color figure can be viewed in the online issue, which is available at wileyonlinelibrary.com.]

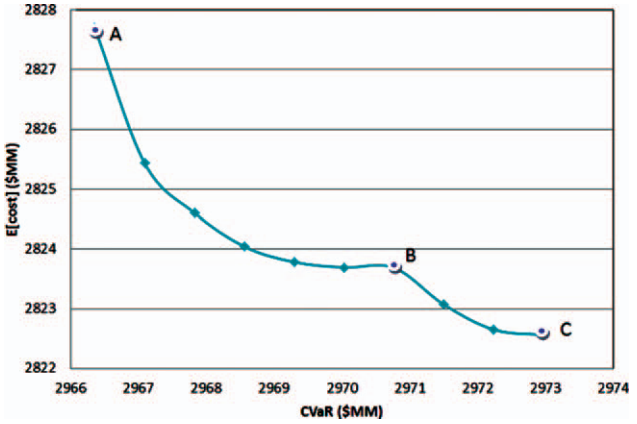

Figure 19. Pareto curve showing economic and risk management of the hydrocarbon biorefinery supply chain.

[Color figure can be viewed in the online issue, which is available at wileyonlinelibrary.com.]

cost ranges from $2822.565 MM (Point C) to $2827.697 MM (Point A), whereas CVaR increases from $2966.367 MM (Point A) to $2972.974 MM (Point C). Pareto design at B is a critical one that the optimal location of biorefineries changes, thus Pareto sets lying between A and B have the same assignment of plants with A while Pareto sets lying between B and C have the same biorefinery sites with C. The unit supply chain cost of hydrocarbon biofuels in designs A, B, and C are $3.36/GEG, $3.355/GEG, and $3.519/GEG, respectively. Their corresponding CVaR are $2966.351 MM, $2968.559 MM, and $2972.974 MM, which shows the trade-off that exist between CVaR and expected annual cost. From Pareto design A to C, the CVaR is increased while the total expected annual cost is reduced. The optimal locations, biorefinery capacities, and selection of technologies are given in Figure 20.

Figure 20c is the optimal supply chain design with the objective of minimizing total expected annualized cost (Point C), and the background is the distribution of population density. The capacities of biorefineries range from 45 MGY to 185 MGY. To reduce the transportation cost, all hydrocarbon biorefineries are built in counties with high demand of hydrocarbon biofuels that can be demonstrated by relatively dense population. Whereas in Figures 20a and b, all hydrocarbon biorefineries are constructed in counties with rich biomass resources. The reason is that the objective of the problem for solutions in Figures 20a and b is minimizing the risk instead of minimizing the total expected cost. Compared to the changes of biofuels demand, variations of supplies are more remarkable because of seasonality. Building a biorefinery in a harvesting site with plentiful biomass resources reduces transportation cost and the risk of supply disruption. The selection of technologies in this case study is identical to the selection in last two case studies, La Salle County is the only county assigned gasification technology; the rest biorefineries are assigned fast pyrolysis as a result of the higher demand of gasoline and better performance of fast pyrolysis on corn stovers.

Results for Multicut L-shaped Method. The size of stochastic programming model is very large, which can be shown in Table 3. Thousand scenarios are required to achieve desired confidence intervals.[40] However, as the number of scenarios increases, the size of model grows

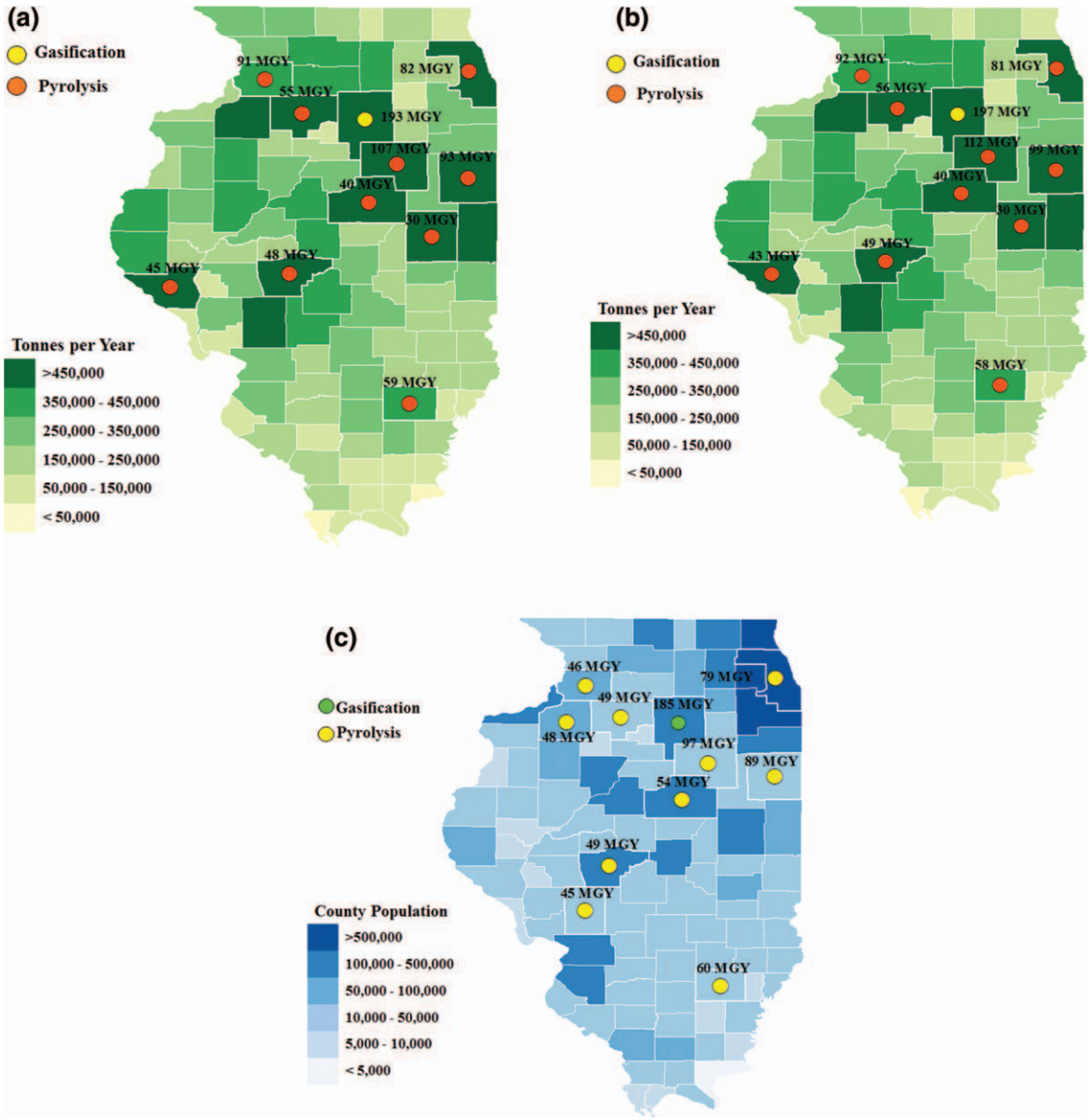

Figure 20. Optimal plant locations, capacities, and selection of technologies for 100 scenarios.

(a) The objective is to minimize CVaR. Background is a map for total biomass distribution (Point A). (b) The objective is to minimize downside risk. Background is a map for total biomass distribution. (c) The objective is to minimize the total expected annualized cost. Background is a map for population distribution (Point C). [Color figure can be viewed in the online issue, which is available at wileyonlinelibrary.com.]

exponentially and as a result the time required for solving the problem increases considerably. It is impossible for CPLEX to solve such a problem directly with a reasonable computational time. Standard L-shaped method and multicut L-shaped method are two effective approaches of reducing time required to solve such type of problems. Figure 21 is a comparison between the two L-shaped methods in terms of the number of iterations in solving 1000 scenarios problem. Standard L-shaped method needs more than 86 iterations to reach the optimal solution, whereas multicut L-shaped method converges after only 24 iterations. Moreover, the two methods are compared in terms of CPU times and the results are shown in Figure 22. Standard L-shaped method needs approximately 8 h to obtain the solution, whereas multicut L-shaped method finds the solution with the same optimality tolerance in 2 h. These two figures demonstrate the computational advantages of multicut L-shaped method: specifically, it requires less iterations and CPU times to find the optimal solution. The main reason is that multicut L-shaped method enforces as many cuts as the number of scenarios at each iteration while standard L-shaped method add only one cut at one iteration. Because of the same reason, multicut L-shaped approach reduces the number of iterations.

Conclusions

This work has introduced a novel decision-support tool for design and planning of a hydrocarbon biorefinery supply chain under supply and demand uncertainty. The problem has been mathematically posed as a multiobjective stochastic programming MILP model accounting for the minimization of the expected annualized cost and CVaR/downside risk. Thus, the model explicitly incorporates the trade-off between financial loss and cost at the decision-making level.

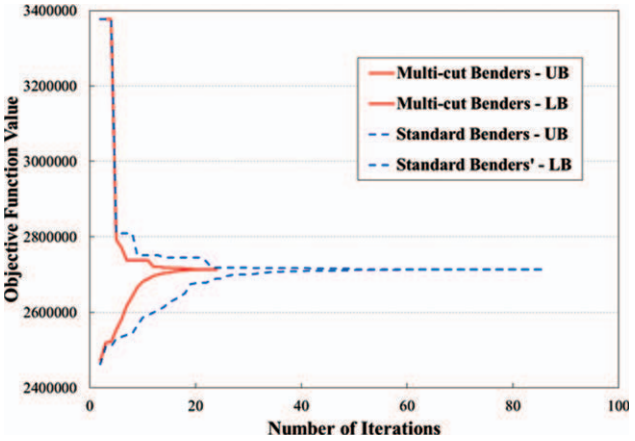

Figure 21. Comparison of two L-shaped methods on the number of iterations.

[Color figure can be viewed in the online issue, which is available at wileyonlinelibrary.com.]

Four case studies for the State of Illinois are presented to demonstrate the effectiveness of the model and algorithm. A comparison between deterministic and stochastic solutions is conducted. When supply and demand change, the stochastic programming model adjusts its solution correspondingly. Thus, the result of stochastic programming model is closer to the reality. Besides, stochastic programming model is looking for a solution that is optimal on average for all scenarios. Deterministic model does not consider uncertainty; its solution is optimal for one case but fail to reach the optimal cost when supply and demand fluctuate. The diverse solutions achieved by the two approaches indicate that deterministic solution is not realistic and effective in the presence of uncertainty.

Next, risk management has been introduced to reduce the risk of high-cost scenarios. Two metrics, downside risk and CVaR, are used and their results are compared. After risk management, total expected cost increases but the risk of high-cost scenarios is reduced. The case study shows, in downside risk management, the probability of low-cost scenarios moves toward the target value Ω. This situation might be improved by changing the target value Ω. However, this is not convenient because finding a suitable target value Ω is not an easy task. This phenomenon demonstrates that downside risk management is highly dependent on the choice of the target value Ω, whereas CVaR does not depend on target value Ω. After CVaR management, the probability of low-cost scenarios does not reduce as much as they behave in downside risk management. So in this specific problem, CVaR management is more convenient and effective than downside risk management.

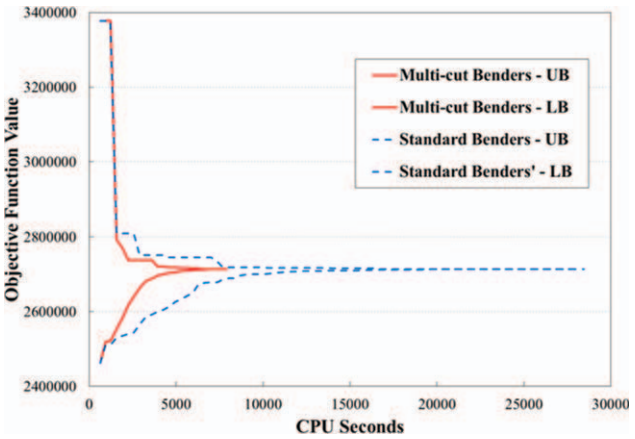

Figure 22. Comparison of two L-shaped methods on CPU seconds.

[Color figure can be viewed in the online issue, which is available at wileyonlinelibrary.com.]

Furthermore, a multicut L-shaped method has been implemented to circumvent the computational difficulties associated with large scale stochastic programming problem. On the computational side, the comparison between the results of the proposed solution strategy and the standard L-shaped decomposition method for the same problem shows that the proposed approach is more efficient. For example: to solve 1000 scenarios problem to its optimality gap of 0.01%, the multicut L-shaped decomposition method requires 2 h CPU times and 24 iterations. However, the standard approach needs 8 h CPU times and 86 iterations to reach the same optimality gap. Multicut L-shaped decomposition method is general enough to be applied to any large scale stochastic programming problem, thus reduces the computational difficulty of practical large scale problems.

Finally, the effectiveness of the proposed approach as a decision-making tool capable of providing valuable insights into the hydrocarbon biorefinery supply chain design problem has been also highlighted. Results indicate that lower levels of risk can be obtained by switching the hydrocarbon biorefineries from locations with high demand to locations with rich biomass. Locations with both high demand and abundant biomass are preferred locations for constructing hydrocarbon biorefineries.

A possible future extension is to perform a nation-level hydrocarbon biorefinary supply chain case study that allows the biomass feedstock and hydrocarbon biofuels to be transported cross the state borders. Another future research path could be accounting for the time-dependent capacity expansion plans and the negotiation between biomass suppliers and biofuel producers.

Acknowledgments

The authors thank the financial support from the Initiative for Sustainability and Energy (ISEN) at Northwestern University and the U.S. Department of Energy under contract DE-AC02-06CH11357.

Notation

Sets/indices

B = set of biomass feedstock indexed by b
I = set of harvesting sites indexed by i
J = set of hydrocarbon biorefinery facilities indexed by j
K = set of demand zones indexed by k
M = set of transportation modes indexed by m
P = set of final products (e.g., gasoline and diesel) indexed by p
Q = set of hydrocarbon biofuel production technologies indexed by q
R = set of capacity levels of hydrocarbon biorefineries indexed by r
T = set of time periods indexed by t, t'
S = set of scenarios indexed by s

Parameters

$\mathrm{BA}_{b,i,t,s}$ = available amount of biomass type b in harvesting site i at time period t for scenario s, kg
$\mathrm{CBM}_{b,i,t}$ = farm-gate cost of biomass feedstock type b from harvesting site i at time period t, \$/kg

$CFJ_{j,q}$ = fixed annual O&M cost as the percentage of the total investment cost of hydrocarbon biorefinery j with conversion technology q.
$CLD_{k,p}$ = local distribution cost of unit quantity of fuel product p at demand zone k, \$/gallon
$CPJ_{j,p,q}$ = net unit production cost per unit quantity of hydrocarbon biofuel type p in hydrocarbon biorefinery j with technology q (after considering byproduct credit), \$/gallon
$CRJ_{j,q,r}$ = total capital investment of hydrocarbon biorefinery j with technology q and capacity level r, \$
$DEM_{k,p,t,s}$ = lower bound of demand for hydrocarbon biofuel product p at demand zones k at time period t for scenario s, gallon
$DFCB_{b,m}$ = distance-fixed cost of biomass type b with transportation mode m, \$/kg
$DFCP_{m,p}$ = distance-fixed cost of hydrocarbon biofuel product type p with transportation mode m, \$/gallon
$DSIJ_{i,j,m}$ = distance from harvesting site i to hydrocarbon biorefinery j with transportation mode m, km
$DSJK_{j,k,m}$ = distance from hydrocarbon biorefinery j to demand zones k with transportation mode m, km
$DVCB_{b,m,t}$ = distance-variable cost of biomass type b with transportation mode m, \$/(kg km)
$DVCP_{m,p,t}$ = distance-variable cost of hydrocarbon biofuel product type p with transportation mode m, \$/(gallon km)
$HBJ_{b,j,t}$ = unit inventory holding cost of biomass type b in hydrocarbon biorefinery j at time period t, \$/(kg day)
H_t = duration of time period t, day
$HPJ_{j,p,t}$ = unit inventory holding cost of hydrocarbon biofuel product type p in biorefinery j at time period t, \$/(gallon day)
HY = production time duration of a year, day
INCM = maximum incentive that can be provided for the construction of biomass conversion facilities, \$
INCP = maximum percentage of the construction cost of biomass conversion facilities that can be covered by government incentive
$INCV_{k,p}$ = volumetric production incentive of hydrocarbon biofuel product type p sold to demand zone k, \$/gallon
IR = discount rate
MC_b = moisture content of biomass type b
NJ_q = maximum number of hydrocarbon biorefineries with technology q that can be constructed
NY = project lifetime in terms of years
PCD = penalty cost of unmet demand \$/gallon
$PRJ_{j,q,r}$ = upper bound of the capacity (in terms of gallons of gasoline equivalent) of hydrocarbon biorefinery j with technology q and capacity level r, gallon
p_s = probability of scenario s
$SJ_{j,t}$ = safety period that should be hold to cover the production shortage in hydrocarbon biorefinery j at time period t, day
$WCIJ_{i,j,m,t}$ = weight capacity for the transportation of biomass from harvesting site i to hydrocarbon biorefinery j with transportation mode m at time period t, kg
$\alpha_{b,p,q}$ = yield of hydrocarbon biofuel product p converted from unit quantity of biomass feedstock type b at hydrocarbon biorefineries with technology q
$\varepsilon_{b,t}$ = percentage of biomass type b deteriorated in storage facility at time period t
$\theta_{j,q}$ = minimum production amount as a percentage of capacity for hydrocarbon biorefinery j with conversion technology q
φ_p = gasoline-equivalent gallons of one gallon of hydrocarbon biofuel product p
ρ_b = mass quantity of standard dry biomass of one dry ton of biomass type b, kg
Ω = target value for risk management, \$
α = confidence level

Integer variable

$x_{j,q,r}$ = 0–1 variable, equal to 1 if a hydrocarbon biorefinery with technology q and capacity level r is located at site j

Continuous variables (0 to ∞)

First stage

$capj_{j,q,r}$ = annual production capacity (in terms of gallons of gasoline equivalent) of hydrocarbon biorefinery j with technology q and capacity level r, gallon
$incj_j$ = incentive received for the construction of hydrocarbon biorefinery j, \$
$tcapj_j$ = total capital investment of installing hydrocarbon biorefinery j, \$
$tcfpj_j$ = fixed annual O&M cost of hydrocarbon biorefinery j, \$

Second stage

$bmp_{b,i,t,s}$ = amount of biomass type b procured from harvesting site i in time period t for scenario s, kg
$fij_{b,i,j,m,t,s}$ = amount of biomass type b shipped from harvesting site i to biorefinery j with transportation mode m in time period t for scenario s, kg
$fjk_{j,k,p,m,t,s}$ = amount of hydrocarbon biofuel product type p shipped from biorefinery j to demand zones k with transportation mode m in time period t for scenario s, gallon
$sbj_{b,j,t,s}$ = storage level of biomass type b in hydrocarbon biorefinery j at time period t for scenario s, kg
$slack_{k,p,t,s}$ = amount of demand for hydrocarbon biofuel product type p that are not met at time period t for scenario s, gallon
$sold_{k,p,t,s}$ = amount of hydrocarbon biofuel product type p sold to demand zones k at time period t for scenario s, gallon
$spj_{j,p,t,s}$ = storage level of hydrocarbon biofuel product type p in biorefinery j at time period t for scenario s, gallon
$wbj_{b,j,q,t,s}$ = amount of biomass type b used for the production of hydrocarbon biofuels through conversion technology q in hydrocarbon biorefinery j at time period t for scenario s, kg
$wpj_{j,p,q,t,s}$ = amount of hydrocarbon biofuel product type p produced through conversion technology q in hydrocarbon biorefinery j at time period t for scenario s, gallon

General

$Cost_s$ = total annualized cost of operating the hydrocarbon biorefinery supply chain in scenario s, \$
$Cost_s^{2stg}$ = second-stage cost of the hydrocarbon biorefinery supply chain scenario s, \$
E[cost] = total expected annualized cost, \$
ψ_s = positive deviation between Ω and cost of scenario s, \$
VaR = value-at-risk, \$
ϕ_s = Positive deviation between VaR and cost of scenario s, \$

Literature Cited

1. Alternative Fuels & Advanced Vehicles Data Center. U.S. Department of Energy, 2012. Available at: http://www.afdc.energy.gov/afdc/fuels/emerging_xtl_fuels.html. Accessed on January 25, 2012.
2. National Acadamy of Science. *Liquid Transportation Fuels from Coal and Biomass: Technological Status, Costs, and Environmental Impacts*. Washington, DC: National Academies Press, 2009.
3. You FQ, Wang B. Life cycle optimization of biomass-to-liquid supply chains with distributed-centralized processing networks. *Ind Eng Chem Res*. 2011;50:10102–10127.
4. Swanson RM, Platon A, Satrio JA, Brown RC. Techno-economic analysis of biomass-to-liquids production based on gasification. *Fuel*. 2010;89:S2–S10.
5. Wright MM, Daugaard DE, Satrio JA, Brown RC. Techno-economic analysis of biomass fast pyrolysis to transportation fuels. *Fuel*. 2010;89:S11–S19.
6. *Annual Energy Outlook 2011*; DOE/EIA-0383(2011); U.S. Energy Information Administration: Washington, DC, 2011.
7. Wright MM, Satrio JA, Brown RC, Platon A, Hsu DD. *Techno-Economic Analysis of Biomass Fast Pyrolysis to Transportation Fuels*. Golden, CO: National Renewable Energy Laboratory (NREL), 2010 (NREL/TP-6A20-46587).
8. Swanson RM, Satrio JA, Brown RC, Platon A, Hsu DD. Techno-Economic Analysis of Biofuels Production Based on Gasification. Golden, CO: National Renewable Energy Laboratory (NREL), 2010 (NREL/TP-6A20-46587).
9. Guillen-Gosalbez G, Grossmann IE. Optimal design and planning of sustainable chemical supply chains under uncertainty. *AIChE J*. 2009;55:99–121.
10. You FQ, Grossmann IE. Design of responsive supply chains under demand uncertainty. *Comput Chem Eng*. 2008;32:3090–3111.
11. Shapiro JF. Challenges of strategic supply chain planning and modeling. *Comput Chem Eng*. 2004;28:855–861.

12. Martin M, Grossmann IE. Energy optimization of bioethanol production via gasification of switchgrass. *AIChE J*. 2011;57:3408–3428.
13. Eppen GD, Martin RK, Schrage L. A scenario approach to capacity planning. *Oper Res*. 1989;37:517–527.
14. Sahinidis NV. Optimization under uncertainty: state-of-the-art and opportunities. *Comput Chem Eng*. 2004;28:971–983.
15. You FQ, Grossmann IE. Multicut Benders decomposition algorithm for process supply chain planning under uncertainty. *Ann Oper Res*. 2011; DOI 10.1007/s10479-011-0974-4.
16. Sokhansanj S, Kumar A, Turhollow AF. Development and implementation of integrated biomass supply analysis and logistics model (IBSAL). *Biomass Bioenergy*. 2006;30:838–847.
17. Bowling IM, Maria Ponce-Ortega J, El-Halwagi MM. Facility Location and Supply Chain Optimization for a Biorefinery. *Ind Eng Chem Res*. 2011;50:6276–6286.
18. Kim J, Realff MJ, Lee JH, Whittaker C, Furtner L. Design of biomass processing network for biofuel production using an MILP model. *Biomass Bioenergy*. 2011;35:853–871.
19. Dunnett A, Adjiman C, Shah N. A spatially explicit whole-system model of the lignocellulosic bioethanol supply chain: an assessment of decentralised processing potential. *Biotechnol Biofuels*. 2008;1:1–17.
20. Zamboni A, Bezzo F, Shah N. Spatially explicit static model for the strategic design of future bioethanol production systems. 2. Multi-objective environmental optimization. *Energy Fuels*. 2009;23:5134–5143.
21. Aksoy B, Cullinan H, Webster D, Gue K, Sukumaran S, Eden M, Sammons N. Woody biomass and mill waste utilization opportunities in Alabama: transportation cost minimization, optimum facility location, economic feasibility, and impact. *Environ Prog Sustainable Energy*. 2011;30:720–732.
22. Elia JA, Baliban RC, Xiao X, Floudas CA. Optimal energy supply network determination and life cycle analysis for hybrid coal, biomass, and natural gas to liquid (CBGTL) plants using carbon-based hydrogen production. *Comput Chem Eng*. 2011;35:1399–1430.
23. Corsano G, Vecchietti AR, Montagna JM. Optimal design for sustainable bioethanol supply chain considering detailed plant performance model. *Comput Chem Eng*. 2011;35:1384–1398.
24. Akgul O, Zamboni A, Bezzo F, Shah N, Papageorgiou LG. Optimization-based approaches for bioethanol supply chains. *Ind Eng Chem Res*. 2011;50:4927–4938.
25. Giarola S, Zamboni A, Bezzo F. Spatially explicit multi-objective optimisation for design and planning of hybrid first and second generation biorefineries. *Comput Chem Eng*. 2011;35:1782–1797.
26. Mele FD, Guillén-Gosálbez G, Jiménez L. Optimal planning of supply chains for bioethanol and sugar production with economic and environmental concerns. *Comput Aided Chem Eng* 2009;26:997–1002.
27. You FQ, Tao L, Graziano DJ, Snyder SW. Optimal design of sustainable cellulosic biofuel supply chains: multiobjective optimization coupled with life cycle assessment and input-output analysis. *AIChE J*. 2012;58:1157–1180.
28. Subrahmanyam S, Peknyt JF, Reklaitis GV. Design of batch chemical plants under market uncertainty. *Ind Eng Chem Res*. 1994;33:2688–2701.
29. Hytoenen E, Stuart PR. Biofuel production in an integrated forest biorefinery-technology identification under uncertainty. *J Biobased Mater Bioenergy*. 2010;4:58–67.
30. Kim J, Realff MJ, Lee JH. Optimal design and global sensitivity analysis of biomass supply chain networks for biofuels under uncertainty. *Comput Chem Eng*. 2011;35:1738–1751.
31. Dal-Mas M, Giarola S, Zamboni A, Bezzo F. Strategic design and investment capacity planning of the ethanol supply chain under price uncertainty. *Biomass Bioenergy*. 2011;35:2059–2071.
32. Marvin WA, Schmidt LD, Benjaafar S, Tiffany DG, Daoutidis P. Economic optimization of a lignocellulosic biomass-to-ethanol supply chain. *Chem Eng Sci*. 2012;67:68–79.
33. National Advanced Biofuels Consortium. Available at: http://www.nabcprojects.org/process_strategies.html. Accessed on January 30, 2012.
34. Verderame PM, Floudas CA. Integration of operational planning and medium-term scheduling for large-scale industrial batch plants under demand and processing time uncertainty. *Ind Eng Chem Res*. 2010;49:4948–4965.
35. Pistikopoulos EN, Ierapetritou MG. Novel-approach for optimal process design under uncertainty. *Comput Chem Eng*. 1995;19:1089–1110.
36. Rooney WC, Biegler LT. Optimal process design with model parameter uncertainty and process variability. *AIChE J*. 2003;49:438–449.
37. Nuernberg R, Roemisch W. A Two-stage planning model for power scheduling in a hydro-thermal system under uncertainty. *Optim Eng*. 2002;3:355–378.
38. Verderame PM, Elia JA, Li J, Floudas CA. Planning and scheduling under uncertainty: a review across multiple sectors. *Ind Eng Chem Res* 2010;49:3993–4017.
39. Gupta A, Maranas CD, McDonald CM. Mid-term supply chain planning under demand uncertainty: customer demand satisfaction and inventory management. *Comput Chem Eng*. 2000;24:2613–2621.
40. You FQ, Wassick JM, Grossmann IE. Risk management for a global supply chain planning under uncertainty: models and algorithms. *AIChE J*. 2009;55:931–946.
41. You FQ, Grossmann IE. Integrated multi-echelon supply chain design with inventories under uncertainty: MINLP models, computational strategies. *AIChE J*. 2010;56:419–440.
42. You FQ, Grossmann IE. Stochastic inventory management for tactical process planning under uncertainties: MINLP Models and algorithms. *AIChE J*. 2011;57:1250–1277.
43. You FQ, Pinto JM, Grossmann IE, Megan L. Optimal distribution-inventory planning of industrial gases. II. MINLP models and algorithms for stochastic cases. *Ind Eng Chem Res*. 2011;50:2928–2945.
44. You FQ, Grossmann IE. Mixed-integer nonlinear programming models and algorithms for large-scale supply chain design with stochastic inventory management. *Ind Eng Chem Res*. 2008;47:7802–7817.
45. Rockafellar RT, Uryasev S. Conditional value-at-risk for general loss distributions. *J Banking Finance*. 2002;26:1443–1471.
46. Uryasev S, Rockafellar RT. *Conditional value-at-risk: optimization approach*. In: Uryasev SPPPM, editor. *Stochastic Optimization: Algorithms and Applications*. Vol. 54, 2001:411–435.
47. Eppen G, Martin R. A scenario approach to capacity planning. *Oper Res*. 1989;37:517–527.
48. Gebreslassie BH, Guillen-Gosalbez G, Jimenez L, Boer D. Economic performance optimization of an absorption cooling system under uncertainty. *Appl Therm Eng*. 2009;29:3491–3500.
49. Carneiro MC, Ribas GP, Hamacher S. Risk management in the oil supply chain: a CVaR approach. *Ind Eng Chem Res*. 2010;49:3286–3294.
50. Van slyke RM, Wets R. L-shaped linear programs with applications to optimal control and stochastic programming. *SIAM J Appl Math*. 1969;17:638–663.
51. Rosenthal RE. *GAMS—A User's Manual*. Washington, DC: GAMS Development Corp., 2011.
52. Searcy E, Flynn P, Ghafoori E, Kumar A. The relative cost of biomass energy transport. *Appl Biochem Biotechnol*. 2007;137:639–652.
53. Mahmud H, Flynn PC. Rail vs truck transport of biomass. *Appl Biochem Biotechnol*. 2006;129–132:88–103.
54. Petrolia DR. The economics of harvesting and transporting corn stover for conversion to fuel ethanol: a case study for Minnesota. *Biomass Bioenergy*. 2008;32:603–612.
55. Eksioglu SD, Li S, Zhang S, Sokhansanj S, Petrolia D. Analyzing impact of intermodal facilities on design and management of biofuel supply chain. *Transport Res Rec*. 2010:144–151.
56. Oracle Crystal Ball. Available at: http://www.oracle.com/us/products/applications/crystalball/index.html. Accessed on January 30, 2012.

Manuscript received Feb. 9, 2012, and revision received Apr. 30, 2012.